



SUB-COMMITTEE ON DANGEROUS
GOODS, SOLID CARGOES AND
CONTAINERS
14th session
Agenda item 10

DSC 14/INF.5
6 July 2009
ENGLISH ONLY

REVISION OF THE CODE OF SAFE PRACTICE FOR SHIPS CARRYING TIMBER DECK CARGOES

Strength of uprights holding timber deck cargoes - formulas and model tests

Submitted by Finland

SUMMARY

Executive summary: This document contains a study on the strength of uprights holding timber deck cargoes for the revision of the Code of Safe Practice for Ships Carrying Timber Deck Cargoes. The study is made by Philippe Chanfreau, The Maritime Academy of Åland University of Applied Sciences, Finland. The Maritime Academy concentrates in this study on the task of determining formulas for the required strengths of stanchions holding timber deck cargoes.

Strategic direction: 5.2

High-level action: 5.2.3

Planned output: 5.2.3.1

Action to be taken: Paragraph 4

Related documents: DSC 12/14; DSC 13/11, DSC 13/WP.3, DSC 13/INF.5 and DSC 14/10

Introduction

1 The Sub-Committee at its 12th session considered document DSC 12/14 (Sweden), which provided a framework and a schedule for the revision of resolution A.715(17) on the Code of Safe Practice for Ships Carrying Timber Deck Cargoes, and agreed that this is an important topic and that Sweden had provided a useful way forward.

2 The Maritime Academy of Åland University of Applied Sciences, Finland, is participating in the revision of the Code concentrating on the task of determining formulas for the required strengths of stanchions holding timber deck cargoes.

For reasons of economy, this document is printed in a limited number. Delegates are kindly asked to bring their copies to meetings and not to request additional copies.



3 This document contains an exhaustive study on the strength of uprights holding timber deck cargoes for the Revision of the Code of Safe Practice for Ships Carrying Timber Deck Cargoes.

Action requested of the Sub-Committee

4 The Sub-Committee is invited to note the information provided.

ANNEX

On the Strength of Uprights holding Timber Deck Cargoes

Formulas and model tests



Research report as part of the TIMRA project and within the framework of
the revision of the IMO Timber Deck Code

17 June 2009

Åland Maritime Academy

Philippe Chanfreau

Åland University of Applied Sciences, Högskolan på Åland

Navigationsskolegränd 2, Mariehamn, Åland Islands, Finland

philippe.chanfreau@ha.ax, www.ha.ax

Contents

1 INTRODUCTION	4
1.1 PREAMBLE	4
1.2 PROPOSED FORMULAS FOR THE STRENGTH OF STANCHIONS HOLDING TIMBER	4
1.3 SHORT OVERVIEW OF THE REPORT	4
2 STANCHIONS FOR ROUND TIMBER	6
2.1 PRACTICAL TESTS, A SHORT INTRODUCTION	6
2.1.1 <i>Equipment</i>	6
2.2 BASIC CONCEPTS AND SOME OF THEIR VALUES DERIVED THROUGH MODEL TESTS	8
2.2.1 <i>The relation between acceleration and inclination in the tests</i>	8
2.2.2 <i>The determination of the friction coefficient μ</i>	8
2.2.3 <i>The angle of repose and the slide angle</i>	9
2.2.4 <i>The force distribution and the centre of impact on the stanchions</i>	12
2.3 MODEL INCLINATION EXPERIMENTS	15
2.3.1 <i>Results from the inclination test with round timber</i>	15
2.4 THE THEORETICAL DERIVATION OF FORMULAS	18
2.4.1 <i>The base formula</i>	18
2.4.2 <i>The main formula</i>	20
2.4.3 <i>Summary of the results for round timber</i>	21
3 STANCHIONS FOR TIMBER PACKAGES	24
3.1 LABORATORY EXPERIMENTS WITH MODEL TIMBER PACKAGES	26
3.1.1 <i>Equipment</i>	26
3.1.2 <i>Determination of the friction between the packages and the supporting surface</i>	27
3.2 MODEL 1: TIPPING OF FORM STABLE TIMBER PACKAGES	28
3.2.1 <i>Experiments with the “Domino Model”</i>	28
3.2.2 <i>Derivation of a formula</i>	30
3.2.3 <i>The formula for tipping stacks of packages: Model 1</i>	32
3.3 MODEL 2: FIRM PACKAGES SLIDING TRANSVERSALLY	34
3.3.1 <i>Model tests with transversally sliding packages</i>	34
3.3.2 <i>Force distribution of timber packages against uprights</i>	35
3.3.3 <i>A theoretical approach</i>	37
3.3.4 <i>The interaction between individual packages</i>	38
3.3.5 <i>The formula for transversally sliding packages: Model 2</i>	39
3.4 MODEL 3: COUNTING WITH NON-FIRM TIMBER PACKAGES	40
3.4.1 <i>Deformed packages and collapsed packages</i>	40
3.4.2 <i>Determination of internal friction of packages with poor form stability</i>	41
3.4.3 <i>Determination of the racking strength of the packages</i>	42
3.4.4 <i>Racking strength as a function of the super positioned load</i>	45
3.4.5 <i>Deformation of timber packages as a function of their position in the stow</i>	48
3.4.6 <i>Inclination tests with a variable number of stacks of deformable packages</i>	50
3.4.7 <i>A theoretical approach on the “soft” packages: Model 3</i>	51
3.4.8 <i>The formula for deformable packages</i>	54
3.5 DISCUSSION HOW TO DETERMINE THE STRENGTH OF UPRIGHTS HOLDING TIMBER PACKAGES	54
4 REFERENCES	57
4.1 SPECIAL THANKS TO	57

1 Introduction

1.1 Preamble

The *Maritime Academy of Åland University of Applied Sciences* is participating in the TIMRA-project in cooperation with MariTerm AB under the leadership and coordination of the Swedish Maritime Administration in the preparation of the revision of the IMO *Code of Safe Practice for Ships carrying Timber Deck Cargoes*.

The Maritime Academy is concentrating on the task of determining formulas for the required strengths of stanchions holding timber deck cargoes.

Within the TIMRA project practical tests in full scale were performed with typical timber deck cargoes in order to investigate their behaviour and characteristics. Tests were performed with both round wood and square sawn timber packages in February 2008 at SCA Transforrest's facilities in Sundsvall, Sweden. See separate report http://www.mariterm.se/TIMRA/TIMRA_Practical_Tests_with_Timber_Cargoes.pdf.

The Maritime Academy managed model tests simulating timber deck cargoes during February – May 2008. The tests were performed in the Åland UAS's facilities in Mariehamn, Åland Islands. These results and the results from the Sundsvall full scale tests in February 2008 serve as a basis for the theoretical derivation of formulas. Further developing the model equipment and further testing was performed in January – June 2009 to gain more knowledge and in order to develop, derive and verify the formulas.

1.2 Proposed formulas for the strength of stanchions holding timber

Through model inclination tests dominant features in the observed dynamics are noted and subsequently modelled. In this study the aim was in the beginning to look for simple manageable formulas. This was the intention, but during the work some formulas have become more and more complex. The dynamics in a stow of timber can be very complex and new elements just tend to come creeping into the formulas. The aim shifted from simplicity to looking for the truth. The object has been to model the real thing as closely as possible and to describe the results and the observations in an understandable way. I believe we are close to the former and it is left to the reader to judge the latter.

1.3 Short overview of the report

Chapter 2 deals with cargos of round timber and contains an introduction to the testing equipment that has been developed simultaneously with the testing and deriving of formulas. Some basic concepts are defined in section 2.2 and at the same time some model testing is carried out to determine some of the basic values needed to understand the results further on. Section 2.3 contains the model tests that are the basis for the derivation of the actual formulas. And finally section 2.4 contains the derivation of the two formulas for the required strength for stanchions holding round timber: the Base formula for small accelerations, that is good

weather conditions and sheltered waters; and the Main formula meant for longer voyages and rougher weather.

A lot of effort put into understanding the special qualities of a stow of logs, such as the slide angle and the force distribution against the uprights.

Chapter 3 deals with cargoes of timber packages. An attempt to outline the vast variety of different situations is made. Section 3.1 presents some of the equipment specially put together for this purpose. The following is concentrated on three possible models. Model 1: tipping of form stable timber packages, Model 2: sliding of form stable packages and Model 3: taking in account the effect of packages with poor form stability (“soft” packages). Model testing is undertaken for all three models. For each model a specific formula is derived using both the results from the tests and rules from physics.

Special qualities of timber packages both alone and in a stow is thoroughly investigated by observing and measuring the model timber packages. Investigated qualities were among others:

- The friction between tiers and on top of the supporting surface
- The racking strength and the inner friction of a package with or without super positioned load,
- The force distribution between sliding packages and uprights,
- Deformation of packages depending on their position in the stow.

Furthermore some qualities that are very specific for a stow of sawn timber packages but difficult to measure are observed and discussed, such as: the interaction between packages resulting in a lowering of the force distribution and the shortening of the retaining lever.

Since a draft to this report was sent to the correspondence group in February this year chapter 3 about timber packages has been rewritten and many subsections have been added. Chapter 2 about round timber is very much unchanged except from some substituted pictures and small formal changes in the resulting formulas.

2 Stanchions for round timber

2.1 Practical tests, a short introduction

The inclination test with round timber in Sundsvall, gave much important information on the features in the dynamics of a stow of round timber. This called for the need to build a model for further tests.

A simple test equipment for similar tests in a scale 1:10 was built up at the Åland University of Applied Sciences during the spring months of 2008. The setup is similar to that in Sundsvall. Accordingly the lower uprights are attached with hinges at their bases and with “hog lashings” with dynamometers. The purpose of the dynamometers and the height where they are attached is to determine the required bending moment of the stanchions. The scale was put to 1:10 for practical reasons and thus the model length measuring unit is decimetres (dm) and the weight measuring unit is kilograms (kg), corresponding to meters and tons in the full scale. Some of the results from the full scale tests in Sundsvall, Sweden are being referred to from time to time in this text.



Figure 2.1.1 a) The setup in Sundsvall and b) the model setup in the Åland Maritime Academy.

2.1.1 Equipment

The test platform is a flat shelf of painted metal mounted on top of a reversed wooden table (see figure 2.1.1b). The lower uprights are mounted with hinges. On top of the stow horizontal ropes with dynamometers connect the lower uprights with the firm upper ones. Later the platform was enhanced by attaching it to the supporting table with hinges (figure 2.2.1). In the first tests the model logs were 3.0 dm long and had a diameter of 0.2 – 0.55 dm. The model logs were predominantly from deciduous trees. The model was enhanced on the 13th of January 2009 by collecting used Christmas trees that people traditionally get rid of that date. So a considerable number of coniferous model logs (figure 2.1.2) of length 50 cm and diameter of 0.2 – 0.6 dm was added to the test setup.



Figure 2.1.2 *The model logs. The deciduous ones of February 2008 at left and the coniferous ones of January 2009 at right.*



Figure 2.1.3 *Dynamometers displaying tension in kilograms ranging up to 23 kg.*

2.2 Basic concepts and some of their values derived through model tests

Some basic concepts will be defined and investigated for the particular test setups in this section.

2.2.1 The relation between acceleration and inclination in the tests

In the tests the accelerations in a real situation are simulated using inclination. In accordance with SJÖFS 2008:4 of the Swedish Maritime Authority the relations between the accelerations (horizontal a_h and vertical a_v) in a real situation and the test inclination angle α are:

$$a_t = \sin \alpha \quad \text{and} \quad a_v = \cos \alpha$$

With *vertical acceleration* is generally meant acceleration *perpendicular* to the deck surface. These equations are used in the derivation of formulas below.

2.2.2 The determination of the friction coefficient μ

The static friction coefficient between the wood and the under lying surface is determined using the commonly known formula

$$\mu = \tan(\rho) \quad \text{which results in} \quad \rho = \arctan(\mu).$$

Where $\alpha = \rho$ is the smallest inclination angle that causes the wood to slide. The value of ρ can typically be in the vicinity of 20 degrees for logs sliding on painted metal. The kinetic friction coefficient is generally counted as 70% of the value of the static friction coefficient.

Tests to determine the static friction coefficients

Tests were carried out with the model logs in order to determine the friction coefficient against the supporting surface. Five model logs were placed on the surface oriented longitudinally or transversally (blocked not to roll) to the inclination direction. The inclination angle was increased slowly until the logs started to slide. The result can be seen in table 2.1. The biggest and the smallest of the inclination angles were omitted and then the average of the middle values was calculated.

Friction test with model logs

test nr	condition	kind of wood	surface	Orientation	first logs to slide (degrees)	last logs to slide (degrees)	average (degrees)	average of middle values	friction coeff. μ
1	dry	deciduous	painted metal	longitudinal	15	25	20		
2	dry	deciduous	painted metal	longitudinal	22	22	22	21	0,38
3	dry	deciduous	painted metal	longitudinal	20	27	23,5		
4	dry	deciduous	painted metal	longitudinal	20	20	20		
5	fresh & sticky	coniferous	painted metal	transversal	26	26	26		
6		coniferous	painted metal	transversal	22	22	22		
7		coniferous	painted metal	transversal	20,5	20,5	20,5		
8		coniferous	painted metal	transversal	20,5	20,5	20,5		
9		coniferous	painted metal	transversal	22	22	22	21,5	0,39
10		coniferous	painted metal	longitudinal	21,5	24,5	23		
11		coniferous	painted metal	longitudinal	19	26	22,5		
12		coniferous	painted metal	longitudinal	25	26	25,5		
13		coniferous	painted metal	longitudinal	24	25,5	24,75	24,4	0,45
14		coniferous	painted metal	longitudinal	24,5	27	25,75		

Table 2.1

Although the transversally placed logs (tests 5 to 9) were prevented from rolling they might have moved a little bit and thus switched from static to kinetic friction and resulted in a lower coefficient than the longitudinally placed ones. In fact this would probably be the case for the bottom logs in a stow subject to transversal acceleration in rough weather.



Figure 2.2.1. Friction tests with a) longitudinally and b) transversally placed logs.

2.2.3 The angle of repose and the slide angle

With little or no inclination a limited section of the logs would slide if the uprights were removed. The impact of this section on the uprights is relatively limited. Experiments and experience show that the *angle of repose* for a stow of logs at 0° degrees of inclination is roughly 45°. The *angle of repose* is the angle between the horizontal plane and the line between the logs that will slide down and the ones remaining. In this paper the complement angle - the angle measured from the vertical line (the removed uprights) – is called the “*slide angle*”. And the cross section of the logs that are expected to slide is called the “*slide triangle*”. When there is a list the *angle of list* is added to the *slide angle* and thus the *slide triangle* grows bigger, (see figure 2.2.2 right).

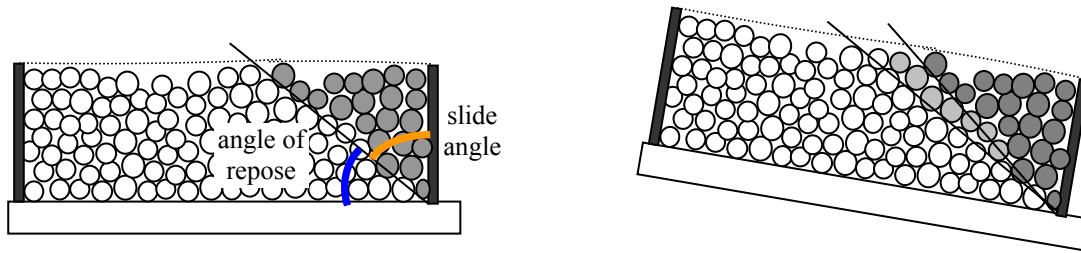


Figure 2.2.2. An illustration of the section of logs contained in the slide triangle.

Tests for angles of repose

In the test performed in February and March 2008 dry model logs of birch and other deciduous trees were used. The model logs were stowed between the uprights and then the uprights on one side were removed and a portion of logs slid down. The angle of repose was measured. In every test the model logs were laid differently, as much as possible simulating a real loading procedure. Pictures from some of the tests are displayed in [figure 2.2.3](#) and the numerical results are presented in Table 2.2 below.



Test nr 3: The slide angle is 51° from the vertical line.



Test nr 5: The slide angle is 45° to 55° from the vertical line.



Test nr 6: The slide angle is 36° from the vertical line



Test nr 7: The slide angle is 41° to 60° from the vertical line

Figure 2.2.3

Tests to determine the angle of repose					degrees from the vertical line	omitting the biggest and the smallest values	omitting the 2 biggest and the 2 smallest values	the middle values of the setups with H = 4 dm
test number	B (dm)	H (dm)	degrees from the horizontal line	mean				
1	6	4	47	47	43	43	43	
2	6	4	48	48	42	42	42	
3	6	4	39	39	51	51		
5	5,5	4	35	45	40	50	50	
6	5,5	4	54	54	36	36		
7	8	3	30	49	39,5	50,5	50,5	
8	8	3	38	38	52			
9	8	3	60	70	65			
			30	30	60			
mean of the remaining slide angles ($^\circ$):					45,4	46,4	45,0	

Table 2.2

The results from the angle of repose tests are presented in the table above. The result from the test number 4 was lost. In test number 9 very few logs first fell, but after a cough the subsequent log slide resulted in an angle 60° from the vertical line. Anyway this test number 9 can be omitted from the average either for giving too big a value or too small a value. A higher stow apparently gives more even results. The last column in table 2.2 displays only the tests with high stows (H = 4 dm). At any rate the tests show that the slide angle is between 45,0 and 46,4 degrees depending on the way to count. Thus the *angle of repose* in average is very close to 45 degrees as assumed.

2.2.4 The force distribution and the centre of impact on the stanchions

Where is the centre of impact for the logs on the stanchions? And what shape does the force distribution (pressure distribution) have in various situations? There are strong reasons to distinguish between the cases 1) where there is little or no inclination and 2) where the inclination is past the point where the logs start to slide. There are several suggestions out of which it is not clear for some what case they are intended for:

- The stack of logs would act like a liquid and thus have a triangular force distribution on the stanchions with the strongest impact at the bottom. In that case the centre of impact would be at one third of the height of the cargo. (For example: Reference 2.)
- A simple assumption that the force distribution is rectangular and thus the centre of impact is at half of the height of the cargo.
- Karpovich, Karpovich, Voynarovskiy (Reference 3) suggest a force distribution which places itself between the two above mentioned. The centre of impact may be at about 40 % of the height of the stanchions.
- A suggestion based on experiments with model logs and soft foam with no inclination.
- A result based on an experiment with model logs and stiff foam and with increasing inclination. The trapezoidal distribution

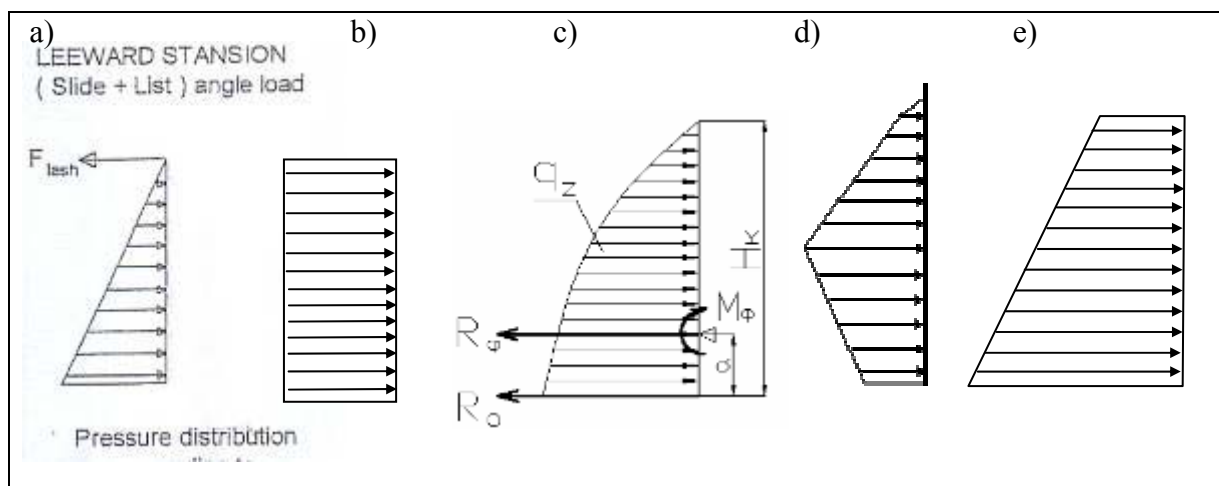


Figure 2.2.4 Various suggested force distributions sketched in the above cases.

Case 1: Force distribution for a stow of logs without inclination

Intuitively alternative c) seems to be the most reasonable when there is no inclination. However experiments with soft foam show that the centre of impact is roughly at half the height of the stanchions and that the force on the bottom is not the maximum of the distribution (see figure 2.2.5). So a possible force distribution could be alternative d), which would fulfil the above mentioned characteristics. Anyway, assuming the centre of impact at half the height is a simple result which will keep us on the safe side even if the force distribution would vary in different situations, which it surely does.



Figure 2.2.5. Model tests that imply that the centre of impact of the slide triangle is roughly at half the height of the stow.

The above discussion about the force distribution applies when the supporting surface is horizontal. When the inclination increases and especially when it is bigger than $\rho = \arctan(\mu)$, i.e. when the logs start sliding on top of the supporting surface, the picture alters.

Case2: Development of the force distribution subject to increasing inclination

Stiff foam was placed between the logs and the uprights. The piece of foam had thickness 105 mm and width 180 mm. The model logs were mostly spruce of 4.8-5.0 dm of length and diameter 0.2-0.6 dm. The weight of the cargo was 58 kg. Between the spruce logs were placed equally sized "contact logs" numbered from I to VIII (from down up), see figure 2.2.6! Table 2.3 shows the distance between each contact log and the supporting board at the other side of the foam. The measured distances were adjusted by subtraction, so that they all start from 100 mm at 0° inclination, before plotting in figure 2.2.7.



Figure 2.2.6 Force distribution tests at 0, 33 and 49 degrees with an example of difference in distance.

Inclination test to determine the shape of the force distribution at different angles																				27.1.2009					
Equally sized "contact logs" numbered from I to VIII (from down up), see pictures!																									
The table shows the distance between each contact log and the supporting board at the other side of the foam																									
Log nr.	I			II			III			IV			V			VI			VII			VIII			
	angle	W	E	average	W	E	average	W	E	average	W	E	average	W	E	average	W	E	average	W	E	average			
0	106	114	110	110	109	110	104	109	107	102	109	106	105	105	105	104	107	106	106	106	108	107	106	105	106
8	106	114	110	107	108	108	103	108	106	101	108	105	104	104	104	104	106	105	105	105	108	107	106	105	106
14	105	114	110	108	106	107	103	106	105	101	106	104	104	104	104	106	105	105	105	105	107	106	106	104	105
20	104	114	109	107	105	106	102	105	104	100	106	103	103	103	103	106	105	105	105	107	106	106	106	103	105
24	104	112	108	107	104	106	102	104	103	99	104	102	102	102	102	104	103	104	103	104	107	106	105	101	103
28	101	108	105	112	102	107	101	100	101	96	102	99	99	99	99	102	101	103	105	104	103	104	99	101	102
33	92	99	96	105	106	106	99	93	96	90	97	94	93	94	94	95	97	96	99	101	100	103	97	100	100
36	83	93	88	98	101	100	93	87	90	85	92	89	88	90	89	92	94	93	96	99	98	101	94	98	98
40	72	79	76	87	88	88	83	75	79	76	82	79	80	82	81	87	86	87	91	91	91	97	89	93	93
43,5	42	58	50	61	70	66	61	58	60	54	66	60	60	67	64	71	74	73	77	81	79	86	81	84	84
47	32	43	38	52	55	54	51	46	49	46	55	51	51	58	55	66	66	66	72	73	73	82	75	79	79
49	21	36	29	40	47	44	41	40	41	36	49	43	45	52	49	60	61	61	66	71	69	78	71	75	75

Table 2.3.

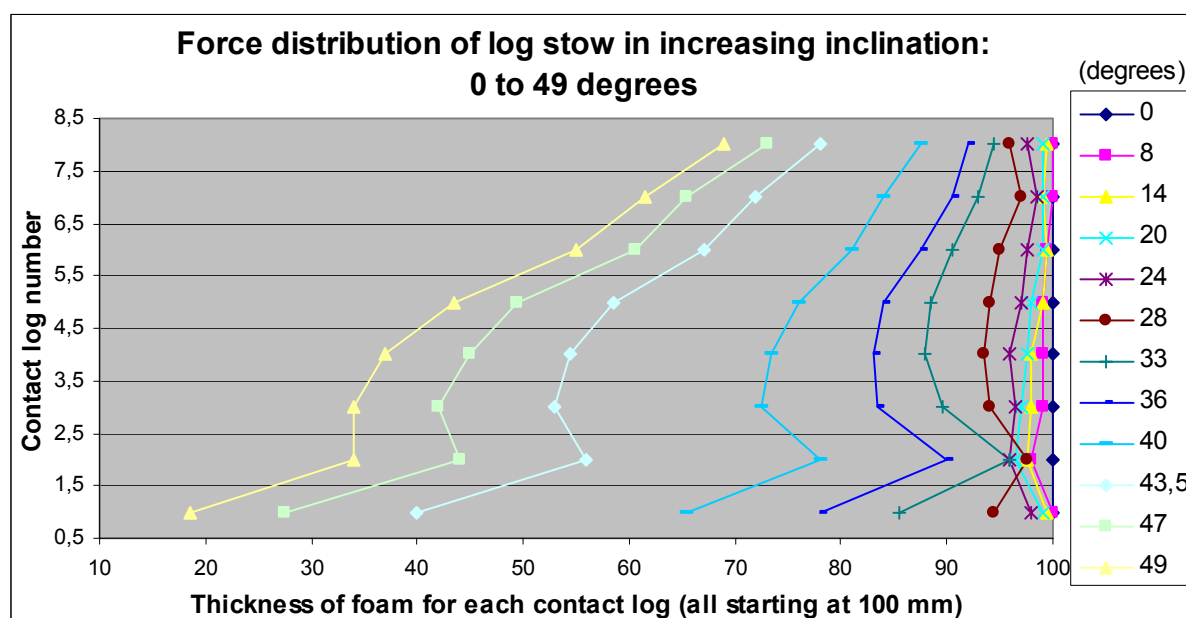


Figure 2.2.7

This test was very time consuming so it was made only once. The result is dependent very much on how each individual (contact) log happens to lay. Apparently contact log number II had a void space behind it and did not advance as much as expected. Number I in turn might have been pushed a little more because of that. Disregarding those irregularities it seems without much doubt that with increasing inclination the force distribution gets approximately the shape of a trapezoid, *Figure 2.2.4 e*, although a cross-breed of c and e cannot be out-ruled. There is not much to be learned from smaller inclination angles in this particular test since this foam was very stiff. But one can clearly see the huge difference of impact between small inclination angles and big ones (corresponding to small accelerations and big ones). The height of the centre point of the force distribution seems to go down to 42% of the cargo height (the height of the contact logs), but on the other hand logs on top tend to roll towards the stanchions on top of the contact logs and thus the results from the higher inclinations should be taken with some reservation (see figure 2.2.6 at right). A calculation of the centre of the force distribution for each inclination angle, counting the first log to be at height 0.5 and

the eighth log at 7.5, results in table 2.4. A good estimation is counting with 45 % of the height.

inclination angle (°)	height of center point of forces	
	(in log diameters)	(in %)
14	3,4	42 %
20	3,4	42 %
24	3,7	46 %
28	3,9	48 %
33	3,7	46 %
36	3,5	44 %
40	3,4	43 %
43,5	3,4	42 %
47	3,4	42 %
49	3,4	42 %

Table 2.4 The calculated height of the centre in the force distributions with increasing inclination.

Results from the force distribution tests

When there is no inclination (case 1), tests pictured in figure 2.2.5 suggest that the biggest force from the log stow is at half the height. When the stow is inclined steeply the test results in an approximation of the centre of impact at 45 % of the height of the stow.

2.3 Model inclination experiments

The tests were carried out as follows. The logs were stowed on top of the flat surface between the uprights. The ropes were mounted with dynamometers. The inclination was increased stepwise and the readings on the dynamometers were noted. On the lower side (when the test surface is inclined) there are uprights mounted on hinges, these are in the following called “low uprights” or “downward uprights”. At the other end of the test surface the uprights are called “high uprights” or “upward uprights”. Uprights are sometimes called stanchions.

2.3.1 Results from the inclination test with round timber

The first two tests were not successful due to the fact that all uprights were too flexible. Inclination test number 3 had firm lower uprights mounted on hinges and the upper uprights of flexible plastic tubes. After about 20° one could see that the increase in force against the low uprights started to accelerate. When the logs started to compress downwards a void space gradually started to form in front of the high uprights. When the upper uprights that way started to loose their support from the cargo the setup gradually collapsed (at about 34°) as the lower uprights were mounted on hinges. In that respect this exactly corresponds to the result in the full scale test in Sundsvall where the high steel uprights bent when they lost the support from the cargo and the entire setup finally collapsed. In the following firm high uprights were used since they serve as holders for the dynamometers.



Figure 2.3.1 Inclination test nr 3.

Test 4 dynamometer (kg)			
angle	N	S	sum
0	0,6	0,65	1,25
4	0,62	0,69	1,31
13	0,64	0,7	1,34
16	0,68	0,76	1,44
17,5	0,73	0,83	1,56
19,5	0,7	0,84	1,54
22	0,78	0,93	1,71
25	0,95	1,17	2,12
27	1,06	1,28	2,34
27	1,14	1,25	2,39
29	1,42	1,71	3,13
32	1,5	1,81	3,31
35	1,66	2	3,66
38	1,83	2,17	4
41	2,07	2,35	4,42
46	2,45	2,78	5,23
49,5	2,79	3,07	5,86
53	2,95	3,24	6,19
57	3,94	4,19	8,13
58	4,17	4,53	8,7
60	4,53	4,96	9,49
60	5,4	5,8	11,2
60	5,54	5,85	11,39

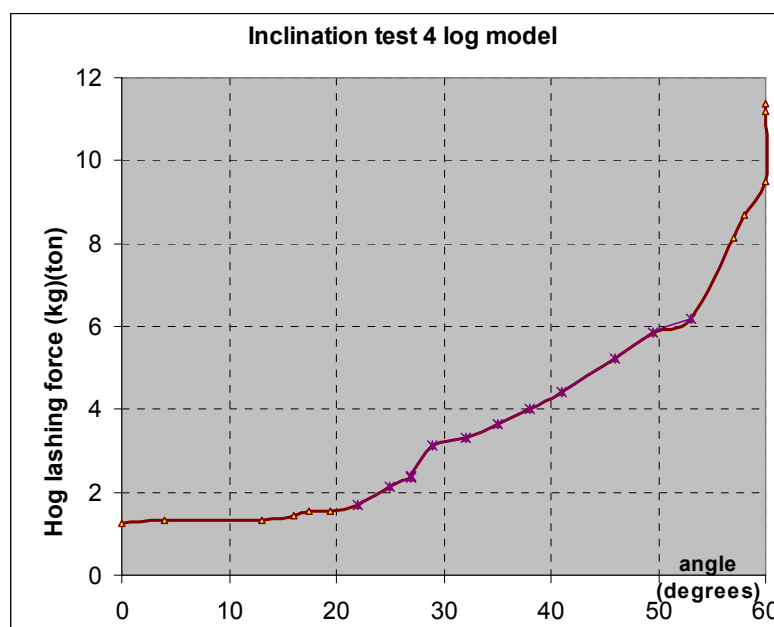


Figure 2.3.2 Inclination test 4.

In inclination test 4 (figure 2.3.2) the high uprights are fixed and almost firm. Thus the readings on the dynamometers should truly show what is happening to the low uprights as a result of the dynamics in the stow when the inclination increases.

Figure 2.3.2 shows the change of behaviour at about 20 degrees of inclination. (Table 2.1 shows that the static friction angle is 21°). There is a linear increase in the force (the shaded numbers in the table, figure 2.3.2) that is faster than before 20° . Obviously it is due to the fact that the static friction force between the logs and the surface is overcome. A third type of behaviour can be seen to appear at about 53 degrees of inclination in this particular setup. What happens there is that the round logs start to “climb” on top of each other and stack at the lower end.

The two main features of this dynamics can be seen also in the graph of figure 2.3.3. Just as test nr 4, tests 5 and 6 show that not much happens between 0 and about 20 degrees. Then there is a linear slope upwards until about $45 - 50^\circ$ after which the slope seems to become steeper.

test 5		test 6	
angle	sum	angle	sum
0	0,92	0	1,37
14	1,14	7	1,07
16	1,36	9	1,14
20	1,58	12,5	1,23
20	1,58	18	1,22
20	1,58	22	1,34
24	2,08	22	1,34
27	2,32	30	2,35
31	2,71	36	3,51
35	3,28	44,5	4,89
37,5	3,62	48,5	7,5
42	5,07	55,5	8,62
47	6,16	61	10,8
47	5,96	64	10,65
51,5	7,41		
51,5	7,09		
57	7,93		
62	9,49		

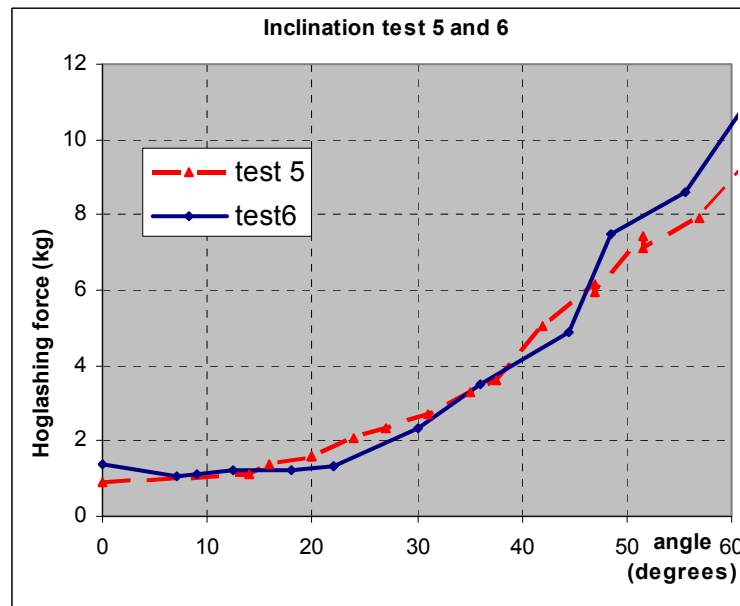


Figure 2.3.3 shows inclination tests 5 and 6.

Conclusions:

Experiments with the scale model show that a stack of round timber loaded between two sets of uprights do not require any extensive force from the uprights as long as the sideward force doesn't exceed the friction between the logs and the supporting surface. The inclination of the test surface - corresponding to the transversal acceleration in the real case – can be increased up to about the angle ρ in the formula $\mu = \tan(\rho)$ (see section 2.2.2). Increasing successively the inclination from 0 to ρ degrees the force on the lower stanchions doesn't increase much. This force is dependent only on the mass and the tendency to move of the timber contained in *the slide triangle*.

When the angle exceeds ρ another behaviour appears: The friction force is exceeded and the entire stow is potentially in motion. The stow is packed against the lower set of stanchions and the upper stanchions begin to lose their support from the logs. When increasing the inclination further the force against the stanchions grows at an increased pace. The two distinctive behaviours could be observed also in the full scale test in Sundsvall the 6th of February 2008. See figure 2.4.5.

Hog lashings that are stretched tighter against the cargo could probably somewhat delay such a “logslide”. Intermediate hog lashings on a lower height would certainly improve the situation – those are not included in this study.

A numerical example: Inclination experiments with logs show that sliding often appears at about 20 degrees, which implies that the static friction coefficient between the logs and the hatch cover is about $\mu = \tan(20^\circ) = 0.36$. Furthermore 20° of inclination should correspond to a transversal acceleration of $a_t = \sin(20^\circ) = 0.34 \cdot g$ or about 3.4 m/s^2 .

Moreover an inclination of 53 degrees corresponds to a transversal acceleration of about $a_t = \sin(53^\circ) = 0.80 \cdot g$ or about 7.8 m/s^2 which corresponds to the

maximal predicted acceleration in the table of transversal accelerations at sea.
Therefore we choose not to propose a separate formula for that range.

2.4 The theoretical derivation of formulas

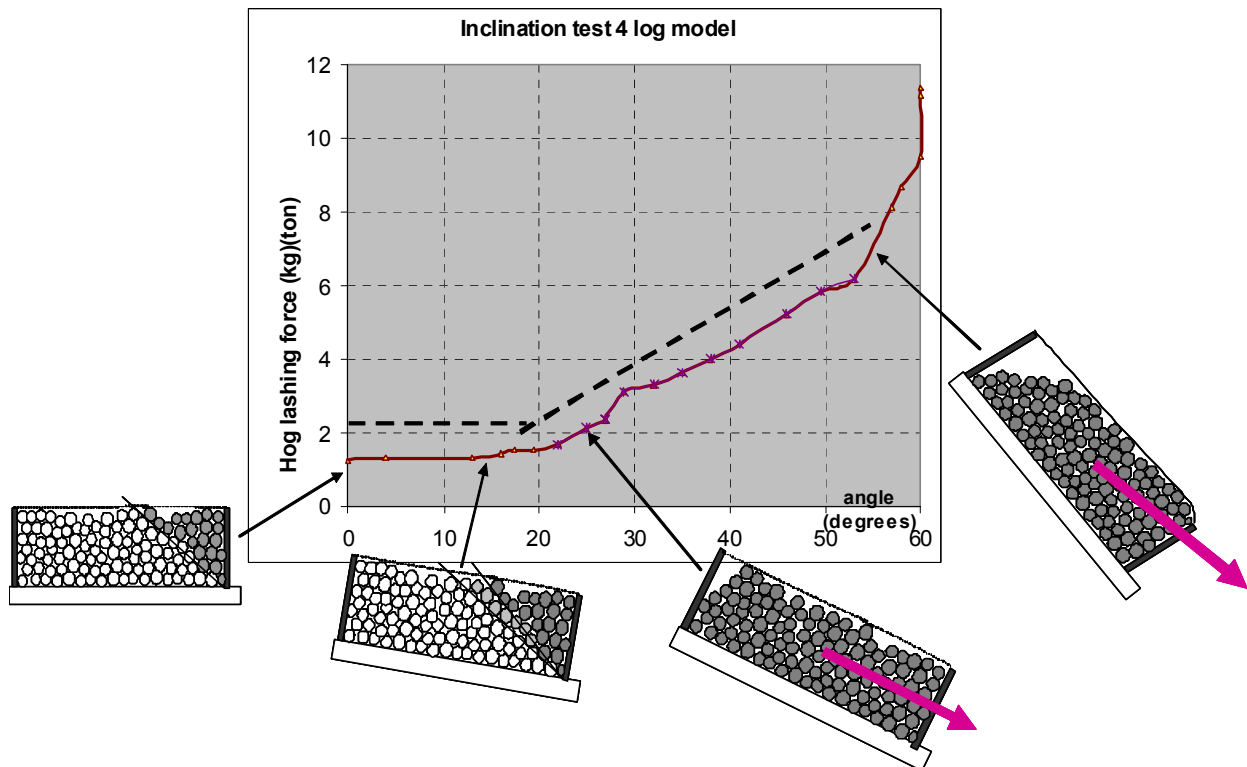


Figure 2.4.1

Figure 2.4.1 shows roughly in pictures what happens to the stow of logs in different stages of inclination. The “active part” of the logs is in grey. Between 0 and 20 degrees nothing much happens. But at about 20 degrees the graph starts to climb almost linearly. The dotted lines are sketches of the models that are about to be derived this section.

2.4.1 The base formula

Experiments show that at small inclination angles (typically between 0 and 20 degrees approximately, or $< \arctan(\mu)$) – corresponding to small accelerations - the forces against the stanchions are fairly small and almost constant up till the point where sliding appears, see figure 2.4.1. That is why the proposed base formula will be a constant with respect to the transversal acceleration.

It is mainly the mass contained in the *slide triangle* that exercises some force. The angle of repose can roughly be set to 45 degrees when the surface is horizontal (see section 2.2.3). How big a force will press against the uprights? That is: how big a portion of the “slide triangle mass”?

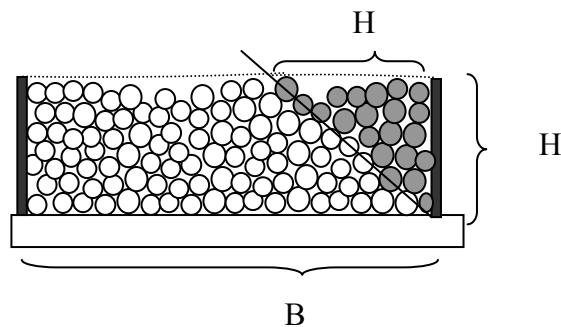


Figure 2.4.2 The slide triangle in relation to the entire stow.

The impact from upward stanchions via possible hog lashings is not counted at this stage – the stanchions have to resist forces standing alone while loading anyway.

In order to fit in a suitable base formula the following assumptions will be made. The slide angle can roughly reach $45 + 20$ degrees (slide angle + list angle) at the most before the logs starting to slide on the hatch surface. Then the cross section of the *slide triangle* has the area $H^2 \cdot \tan(65^\circ) / 2$. The cross section area of the entire stow is obviously $H \cdot B$.

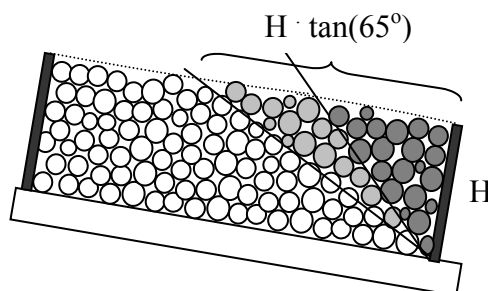


Figure 2.4.13.

Then the maximum portion of the stow that will potentially be in motion before sliding of the whole stow is then $\frac{H^2 \cdot \tan(65^\circ) / 2}{H \cdot B}$ which equals to $\frac{H \cdot \tan(65^\circ)}{2B}$. Then the mass force from the cargo is $\frac{H \cdot \tan(65^\circ)}{2B} \cdot mg$. Assuming this portion of the stow is thought to slide on an imaginary slope of 45° within the stow with a friction coefficient of μ_s , then the force on the stanchions is $Q = \frac{H \cdot \tan(65^\circ)}{2B} \cdot mg \cdot (\sin 45^\circ - \mu_s \cdot \cos 45^\circ)$. Where $\sin 45^\circ$ has to do with the weight component parallel to the 45° slope and $\mu_s \cdot \cos 45^\circ$ has to do with the friction between the moving logs and the motionless ones.

Assuming the centre of impact on the stanchions is at $H/2$: (section 2.2.4)

$$M_b = \frac{H \cdot \tan(65^\circ)}{2B} \cdot mg \cdot (\sin 45^\circ - \mu_s \cdot \cos 45^\circ) \cdot \frac{H}{2} = \frac{H^2}{4B} \cdot mg \cdot \tan(65^\circ) \cdot (\sin 45^\circ - \mu_s \cdot \cos 45^\circ)$$

According to the Sundvall tests the static friction coefficient log-to-log was found to be 0.78 when sliding sideways in wet condition. Whether this is applicable to logs sliding on top of each other transversally is a tricky question. The movement is promoted by the logs tendency to roll but prevented by the fact that the thought “inclined surface” is all but flat. Assuming these characteristics omit each other we settle for the value $\mu_s = 0.7$ and get the

approximation $M_b = \frac{H^2}{B} \cdot mg \cdot 0.12$. This seems to fit the experimental values nicely. In general the base formula could be written as follows, where N is the number of uprights on the same side.

$$M_b = 0.12 \cdot \frac{H^2}{B \cdot N} \cdot mg$$

2.4.2 The main formula

The middle section of the graph in figure 4 is observed to be roughly linear which implies that the dominant feature in the dynamics can be explained by the entire stow of logs moving as a monolith mass. Thus the force upon the lower stanchions should be dominated by

$$Q = mg \cdot \sin(\alpha) - \mu \cdot mg \cdot \cos(\alpha)$$

i.e. the transverse acceleration force (simulated by the component of the gravitational force in the test) minus the friction force between the logs and the under laying surface.

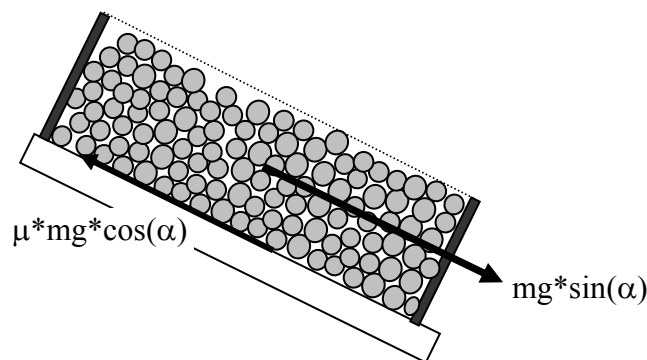


Figure 2.4.4 The forces acting on a stow of round timber moving as a monolith mass.

Converting the inclination to accelerations (with $a_t = \sin(\alpha)$ and $a_v = \cos(\alpha)$) yields:

$$Q = (a_t - \mu \cdot a_v) \cdot mg,$$

Where Q is the total force against the stanchions, a_t = transverse acceleration/g, a_v = vertical acceleration/g, μ = dynamic friction coefficient between the logs and the hatch surface and $g = 9,81 \text{ m/s}^2$. The unit of Q is kN.

As mentioned above an upward stanchion tends to loose its support from the cargo and with hog lashings in place the upward stanchion can support the downward stanchion with the

same moment as the latter – or even less. The impact of lashing flexibility even diminishes the contribution of the upward stanchion. This has not been investigated in detail at this stage but has been added as a coefficient k in the formulas.

The experiments seem to imply that the centre of impact of Q on the stanchions is at about 45 % of their height H (section 2.2.4). With the number of downward stanchions N , the above discussion would lead to the moment equation

$$k \cdot M_b \cdot N = Q \cdot 0.45 \cdot H ,$$

where the factor k ($1 \leq k \leq 2$) is dependent on the way the low stanchions are supported by the high ones. Thus $k = 1$ means there is no support from the high stanchions, $k = 2$ means that the high stanchions support the lower ones via firm lashings but the high ones have no support from the cargo. A flexible lashing would mean a value of k somewhere between 1 and 2. A value $k > 2$ would imply that the high stanchions have a firm support from the cargo and that the hog-lashings are firm and non-flexible. M_b is the total bending moment on the low stanchions.

This results in
$$M_b = 0.45 \cdot \frac{1}{k \cdot N} Q \cdot H \text{ or}$$

$$M_b = \frac{0.45}{k \cdot N} \cdot (a_t - \mu_d \cdot a_v) \cdot mg \cdot H$$

The unit is kNm . If $a_v = 1$ and M_b is given in *ton metres*, then the formula gets the following form

$$M_b = \frac{0.45 \cdot H}{k \cdot N} \cdot (a_t - \mu_d) \cdot m ,$$

which means that M_b is linearly dependent on a_t . N.B. that this formula can be applied for bigger accelerations well past the point where the cargo begins to slide against the hatch surface.

However there are no extra margins nor any assumptions of other features in the dynamics. Taking into account the capriciousness in the dynamics of such a stow under rough conditions it would be reasonable to add a safety margin. This can be done by keeping the coefficient k low.

2.4.3 Summary of the results for round timber

The dimensions for stanchions holding round timber may be calculated using the following formulas:

Formula 1. (the Base Formula) is used for small accelerations corresponding to an inclination $< \arctan(\mu)$, i.e. before the transversal force exceeds the static friction. The factor 1.35 should

be added to allow for the fact that the force from the cargo can (momentarily) press more on one of the stanchion than on the others.

$$M_b = 1.35 \cdot 0.12 \cdot \frac{H^2}{B \cdot N} \cdot mg$$

Formula 2 (the Main Formula) is used for bigger accelerations.

$$M_b = \frac{0.45 \cdot H}{k \cdot N} \cdot (a_t - \mu \cdot a_v) \cdot mg$$

To these formulas should be added the impact of the additional transversal forces, the wind pressure PW and the sea sloshing pressure PS . The additional moment, counting with 45 % of the height of the stow is then $0.45 \cdot H \cdot (PW + PS)$. Furthermore the factor 1.35 should be added.

Formula 2 can then be written:

$$M_b = 1.35 \cdot \frac{0.45 \cdot H}{k \cdot N} \cdot (a_t - \mu \cdot a_v) \cdot mg + 1.35 \cdot \frac{0.45 \cdot H}{k \cdot N} \cdot (PW + PS)$$

The unit is kNm. For given accelerations the one formula that gives the higher value is chosen, that is:

$$M_b = \max(\text{Formula 1}, \text{Formula 2})$$

The used symbols are the following:

H = the height of the cargo (m)

B = the transverse width of the stow

a_t = the transverse acceleration/g

a_v = the vertical acceleration (perpendicular to the deck) /g

μ = the dynamical friction coefficient

m = the mass of the stow (ton)

$g = 9.81 \text{ m/s}^2$

N = the number of uprights on each side of the stow

k = the hog lashing coefficient ($1 \leq k \leq 2$)

PW = Force from wind pressure in kN

PS = Force from sea sloshing in kN

In figure 2.4.5 the formulas are plotted together with the measured values in the full scale tests in Sundsvall, Sweden. The moments of the two stanchions are plotted separately in that graph.

In figure 2.4.6 the formulas are plotted together with three model tests. The moments are plotted in unit $kg \cdot dm$ ($g = 9.81 \text{ m/s}^2$ is omitted). The following values are used: $H = h = 3 \text{ dm}$, $B = 8 \text{ dm}$, $m = 36 \text{ kg}$, $a_v = 1$, $\mu_d = 0.7 \cdot 0.38 = 0.266$ (the dynamic friction) and $k = 1$. There was obviously no effect from wind and sea water in the tests.

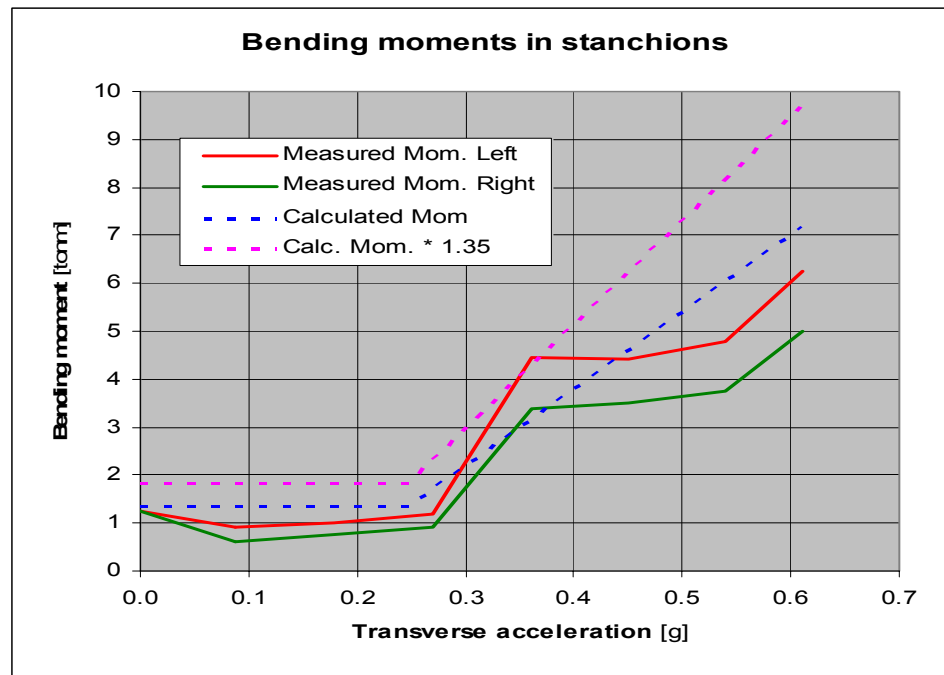


Figure 2.4.5 A comparison between the full scale tests in Sundsvall and the above derived formulas.

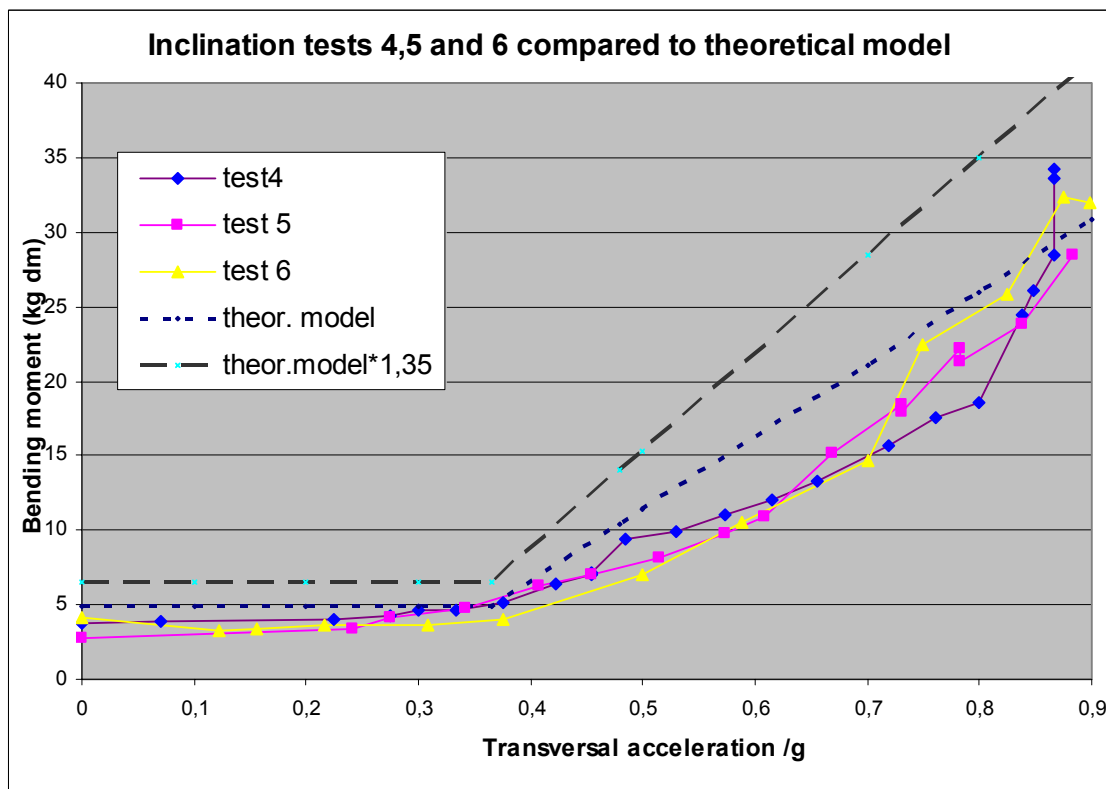


Figure 2.4.6 Fitting the theoretical model to the model test results.

3 Stanchions for timber packages

Looking for a suitable model two extreme theoretical examples are presented in order to outline the frames. Consider a stow of timber packages with the height H .

Model A: The entire stow of timber packages will stay together as a solid box (parallelepiped). A resulting force of $F_a - F_f$, where F_a is an acceleration force and F_f is the friction force against the supporting surface, will push the box against the uprights. The uprights are flexible and will meet the acceleration force at a very low level, as a suggestion at half the height of the bottom tier, i.e. $H/10$. (see figure 3.1) The forces $F_a - F_f$ and F_u are equal in strength but are not on the same line, so possibly the “box” could tip. But it is wide enough so it will not happen. Thus the required moment for the uprights to resist the pushing box is $M = (F_a - F_f) \cdot \frac{H}{10}$.

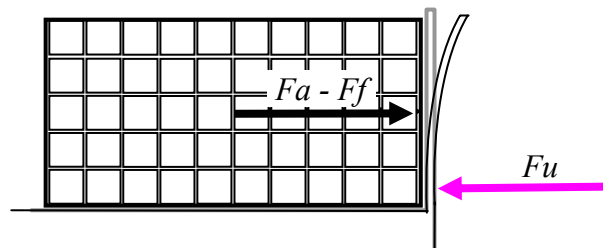


Figure 3.0.1

Model B: (“Worst case”) There are a number of tiers of packages. The tiers of the stow will slide without friction on top of each other. Then each tier will push on the uprights with one fifth of F_a . The uprights will have to respond with a corresponding series of forces point-wise. In general the forces will be uniformly distributed along the uprights, thus the centre of impact is at $H/2$ and the uprights have to respond with a total moment of $M = F_a \cdot H/2$.

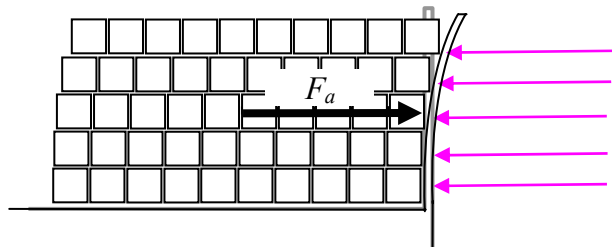


Figure 3.0.2

*A numerical example: Assuming the height $H = 5$ m, the mass $m = 50$ ton, the transversal acceleration $a_t = 0.5$ g and the friction coefficient to be $\mu = 0.3$. Then Model A will require a moment $M = (50 \text{ t} * 0.5 - 0.3 * 50 \text{ t}) * 5\text{m}/10 = 5$ ton meters. Model B would require $M = 50 \text{ t} * 0.5 * 5\text{m}/2 = 62,5$ ton meters.*

In reality the models to be used place themselves between these two extremes. Of course one can always count with friction. But even if the friction between the tiers is sufficient to prevent sliding the friction between the layers within the packages can cause the packages to deform, which in turn causes the entire stow to deform and to press more on the upper parts of the uprights, much as in figure 3.0.2.

Looking for the worst scenario in terms of pressure on the uprights in a realistic case there are several possible scenarios for a stow of timber packages. There are many different ways to

load a stow, depending of the length of the voyage, the weather forecasts, the sizes and the quality of the packages and so forth. When uprights are used it should be customary that at least the packages closest to the uprights are stowed longitudinally. Then various methods for preventing sliding transversally might be applied or not. Obviously it is important to stow the bundles tight and avoid all empty spaces between them. The situation is furthermore dependent on how and to what extent lashings are applied.

Moreover the stability of the stow is dependent on the stability of individual packages, most specifically the ones in the bottom tier and the ones closest to the uprights that are subject to the strongest pressure. If almost all packages of the entire stow have collapsed, due to a combination of reasons that should not be allowed, and the uprights are still standing then the methods for round timber should be applicable. But it is assumed in the following that there is at least some form stability of both the individual packages and the stow.

Basically it is all about the form stability of the stow! As long as the stow stands firm and rectangular almost no bending moment is exerted on the uprights (figure 3.0.1). If/when the stow starts exerting pressure on the uprights that means that forces make the stow become more like a parallelogram and thereby press also on the upper parts of the uprights. This can happen in three ways: The stacks of packages tip (figure 3.0.3) , the tiers of packages slide (figure 3.0.2) or the individual packages become like parallelograms (figure 3.0.4). In fact these three behaviours have been observed to happen simultaneously in the model tests (this can be seen sketched in figure 3.0.4). Nevertheless there is an inner resistance against deformation of both the individual packages and in the entire stow itself. This is the difficult part to model.

In this paper the following models will be investigated.

- **Model 1:** Stacks of rigid packages are blocked vertically from sliding transversally. With increased transversal acceleration the stacks begin to tip against each other and against the uprights. See figure 3.0.3. This possible configuration is investigated in section 3.2.

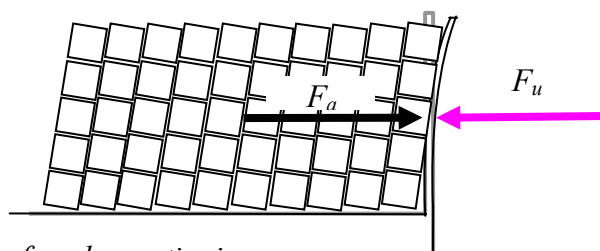


Figure 3.0.3. Stacks of packages tipping.

- **Model 2:** The tiers of rigid packages are able to slide transversally. The uprights have to match the difference between the sideways force and the friction forces between the tiers or between the hatch surface and the bottom tier. See figure 3.0.2. This configuration is discussed in section 3.3.
- **Model 3:** The tiers do not slide, the stacks do not tip. But each package has poor form stability. The layers within each package are able to slide transversally (back and forth) which can alter the form of the package from a rectangle to a parallelepiped with the same height. See figure 3.0.4. Regardless of any applied top over lashings the entire stow will then alter its shape. How does that affect the forces against the uprights? This is investigated in section 3.4.

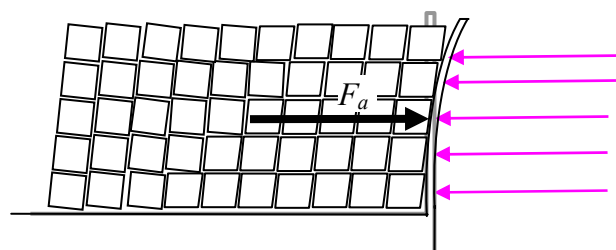


Figure 3.0.4. Individual packages lose their form stability and align uniformly along the bending uprights.

3.1 Laboratory experiments with model timber packages

3.1.1 Equipment

The same test platform with dynamometers as described in section 2.2.1 was used when testing the model timber packages. See figure 3.1.2.



Figure 3.1.1 a) An x-model package b) another x-package deformed. c) A y-model package, “soft version” with masonite and rubber bands. d) y-package deformed.

About thirty-two model timber packages were put together. Some packages are realistic models put together with model boards 400 mm long and 5mm by 15 mm (or 10 by 15) and stickers of 1mm plywood. These are called “x-type” packages. The other packages were put together simply with piles of boards (400 mm long, 100 mm wide and 20 mm thick) with two or three supporting “beams” underneath. These are called “y-type” packages. The y-packages

were tied together with strong strings in their rigid version (section 3.2). The “soft” version was put together by replacing one board with a number of sheets of masonite (figure 3.1.1c). The packages were tied with elastic rubber bands. These versions of the packages were used in the experiments of section 3.4 where their characteristics are further investigated.

3.1.2 Determination of the friction between the packages and the supporting surface

Three packages were put on the test surface. It was observed at what angle the packages started to slide. The angles of the first and the last package to slide were noted. Then three other packages were placed on the surface and so on. Altogether 15 packages were tested this way in 5 identical tests. The average of the first and the last was calculated each time. The biggest and the smallest average values from the tests were omitted and the average of the remaining ones was calculated. The result was that the sliding angle is 17° . Which according to section 2.2.2 corresponds to a static friction coefficient of $\mu = \tan(17^\circ) = 0.31$ (table 3.1).



Figure 3.1.2 a,b,c) Friction tests with model timber packages.



Timber package slide test			
	first	last	average (degrees)
	15	17	16,00
	17	20	18,50
	14	18,5	16,25
	15	31,5	23,25
	14	18,5	16,25
	average		17
$\tan(17^\circ) =$	$\mu =$	0,31	

Table 3.1

Further friction tests were made later in connection with the model 2 experiments. In each experiment three new packages are placed on a surface that is inclined slowly. The angles of inclination are noted when the first, the second and the third package moves. The results are the following:

y-type packages standing on wooden slats					y-type packages standing on painted metal				
	1st	2nd	3rd	median		1st	2nd	3rd	median
1st try:	22	23,5	25	23,5	1st try:	19	19	19	19
2nd try	26	26	26	26	2nd try	15	15	15	15
3rd try	19	27	27	27	3rd try	19	19	19	19
mean: 25,5 degrees					mean: 17,67 degrees				
$\mu = 0,48$					$\mu = 0,32$				
x-type packages standing on wooden slats					x-type packages standing on painted metal				
	1st	2nd	3rd	median		1st	2nd	3rd	median
1st try:	24	24	24	24	1st try:	15	19,5	21	19,5
2nd try	21	24	24	24	2nd try	16	19	19	19
3rd try	22	24,5	24,5	24,5	3rd try	13,5	15,5	17,5	15,5
mean: 24,17 degrees					mean: 18 degrees				
$\mu = 0,45$					$\mu = 0,32$				



Figure 3.1.3 a) Friction test with y-packages on wooden slats b) x-packages on the model hatch surface.

3.2 Model 1: Tipping of form stable timber packages

3.2.1 Experiments with the “Domino Model”

A special case is chosen for the first study on timber packages: the tiers of packages are prevented from sliding on top of each other, for instance by systematically placing vertical boards between the stacks of packages. Horizontal sliding can also be prevented by alternating packages with different heights. In this case the stacks of packages were actually kept separate by the vertical boards and they started leaning against each other with increasing inclination.

Model experiments were carried out in the timber laboratory of ÅUAS, Maritime Academy in the spring months of 2008. Another test series was made in June 2009.

Inclination tests were made with a variable number of stacks standing and leaning against the “stanchions”, supported by hinges at their bases and “hog lashings” with digital dynamometers in the upper ends.



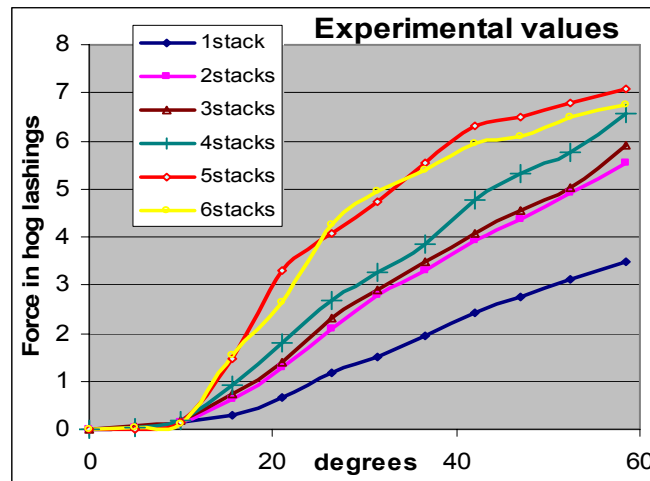
Figure 3.2.1 Model tests with tipping timber packages.

Somewhat surprisingly the expected increase of the force against the stanchions diminishes with each added stack of packages. This can be seen in figure 3.2.2.

This behaviour can be explained by the internal friction between the stacks when each stack is about to tip. With an increasing number of stacks tipping and pushing behind, the internal friction increases even further. The entire stow then acts as a slightly deformed parallelepiped which cannot tip in its entirety. It has to be stressed that this behaviour appears specifically when the individual packages are blocked from horizontal movement and when no racking occurs. In figure 3.2.2 values from a series of experimental inclination tests with variable numbers of package stacks are displayed. Table 3.2 contains the sum of what the two dynamometers showed at different angles. The values were adjusted by subtraction so that all graphs begin at zero.

Angle (°)	1 stack (kg)	2 stacks (kg)	3 stacks (kg)	4 stacks (kg)	5 stacks (kg)	6 stacks (kg)
0	0,36	0,31	0,47	0,55	0,00	0,00
5	0,41	0,33	0,53	0,58	0,00	0,03
10	0,49	0,45	0,67	0,75	0,14	0,10
15,5	0,65	0,95	1,18	1,47	1,48	1,55
21	1,01	1,60	1,84	2,34	3,30	2,64
26,5	1,52	2,40	2,79	3,23	4,08	4,26
31,5	1,88	3,09	3,35	3,80	4,72	4,97
36,5	2,29	3,61	3,94	4,42	5,55	5,40
42	2,77	4,22	4,54	5,34	6,30	5,93
47	3,13	4,69	5,02	5,88	6,51	6,10
52,5	3,49	5,23	5,51	6,32	6,80	6,49
58,5	3,85	5,86	6,39	7,12	7,08	6,75

Table 3.2



Figures 3.2.2: Experimental values from stacks of timber packages tipping. The results are adjusted so that the initial lashing force is put to the same level in the first graph that shows experimental values.

3.2.2 Derivation of a formula

The first stack (the one furthest behind) will get the resulting moment M_1 from a transversal tipping moment $m_s \cdot a_t \cdot \frac{H}{2}$ and a retaining moment $F_N \cdot \frac{b}{2}$:

$M_1 = (m_s \cdot a_t \cdot \frac{H}{2} - F_N \cdot \frac{b}{2})$, where $F_N = m_s \cdot g$ is the normal force (the weight of one stack) and H and b are the height and the width of the stack respectively. When the first stack tilts and pushes on the second with a force $F_{t1} = M_1 \cdot \frac{2}{H}$, the latter will get the following moment:

$$M_2 = (m_s \cdot a_t \cdot \frac{H}{2} - F_N \cdot \frac{b}{2}) + F_{t1} \cdot \frac{H}{2} - F_{f1} \cdot b, \quad \text{or simply} \quad M_2 = M_1 + M_1 - F_{f1} \cdot b$$

where $F_{f1} = \mu_i \cdot F_{t1} = \mu_i \cdot M_1 \cdot \frac{2}{H}$ is the internal friction force between the first two stacks.

Then we can write: $M_2 = M_1 \cdot (1 + (1 - \mu_i) \frac{2 \cdot b}{H})$

Increasing the number of stacks further results in an increasing internal friction further down the line which lead to the parts of the stow sticking better together and means that the impact on the stanchions does not continue increasing proportionally with every added stack.

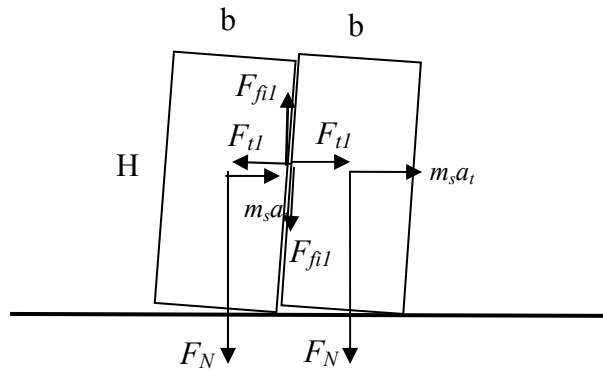


Figure 3.2.3: Forces appearing on and between the two first stacks of timber packages.

The second stack will in turn push the third stack which then gets the following moment:

$M_3 = (m_s \cdot a_t \cdot \frac{H}{2} - F_N \cdot \frac{b}{2}) + F_{t2} \cdot \frac{H}{2} - F_{fi2} \cdot b$ where $F_{fi2} = \mu_i \cdot F_{t2} = \mu_i \cdot M_2 \cdot \frac{2}{H}$ is the internal friction force between the second and the third stack. Substituting the formulas results in

$$M_3 = M_1 + M_2 - \mu_i \cdot M_2 \cdot \frac{2 \cdot b}{H} = M_1 + M_2 \left(1 - \mu_i \cdot \frac{2 \cdot b}{H}\right) = M_1 + M_1 \cdot \left(1 + \left(1 - \mu_i \cdot \frac{2 \cdot b}{H}\right)\right) \left(1 - \mu_i \cdot \frac{2 \cdot b}{H}\right)$$

and results in $M_3 = M_1 \cdot \left(1 + \left(1 - \mu_i \cdot \frac{2 \cdot b}{H}\right) + \left(1 - \mu_i \cdot \frac{2 \cdot b}{H}\right)^2\right)$.

It can then easily be shown that the general formula is:

$$M_n = M_1 \cdot \left(1 + x + x^2 + \dots + x^{n-1}\right) \text{ where } M_1 = \left(m_s \cdot a_t \cdot \frac{H}{2} - F_N \cdot \frac{b}{2}\right) \text{ and } x = \left(1 - \mu_i \cdot \frac{2 \cdot b}{H}\right).$$

Finally the following formula for the n:th stack is obtained by collecting the sum and making some substitutions:

$$(3.2.1) \quad M_n = \frac{mg}{n} \cdot \left(a_t \cdot \frac{H}{2} - a_v \cdot \frac{b}{2}\right) \cdot \frac{1 - (1 - F)^n}{F},$$

where m is the total mass of the stow, n is the number of stacks of packages and $F = \mu_i \cdot \frac{2 \cdot b}{H}$.

Remark: Even if the stack of packages stays perfectly rectangular the lever of the retaining moment (until now assumed as $b/2$) immediately becomes shorter when the stack begins to tip. In fact the stack “has to” tip in order for the internal friction to take effect. The taller the stack, the faster the retaining lever shortens (see figure 3.2.4)! Furthermore, when an acceleration force acts on the stack, the latter tends to “bend forwards” due to slight compression of the boards on the “low” side. The upper packages can also slide a little bit. Or the bottom, or several packages can rack (see figure 3.4.9 centre). All this contributes to displacing the centre of gravity and thus shortening the retaining lever. Finally, as the stack tilts slightly, the centre of gravity raises a little bit from $H/2$, which increases the tipping moment slightly. All this can be dealt with by introducing a reduction factor r on the originally assumed retaining lever: $\frac{b}{2} \cdot r$. The model tests strongly support such an introduction. (see figures 3.2.5 and 3.2.7). And keeping the calculated retaining lever low is

safer than overestimating it! The reduction factor can be set to $0.5 \leq r \leq 1$ depending on the height of the stacks and other characteristics.

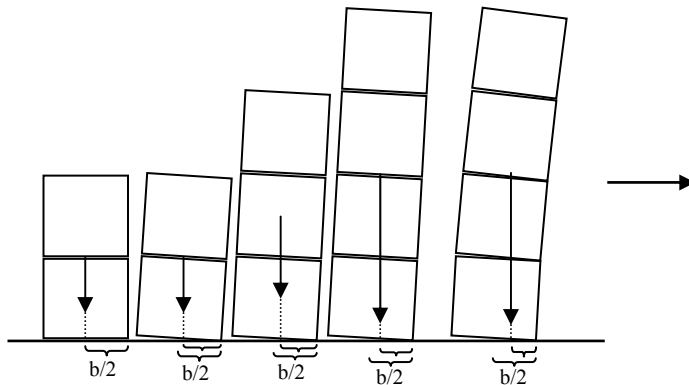


Figure 3.2.4 The retaining lever shortens when the stack of packages tilts and especially when it is higher and/or “bends”.

Furthermore there is an interaction between the individual packages that leads to a lowering of the force distribution on the uprights. The resulting bending moment thus has a smaller lever. This effect is thoroughly discussed in section 3.3.4. This effect can be dealt with by adding an “interaction coefficient” $0.7 \leq C \leq 1$. On the other hand it is risky to add such an assumption to a general formula just on the basis of a series of model tests. Lowering C from $C = 1$ would approach the model to the truth but it would lower a security margin.

3.2.3 The formula for tipping stacks of packages: Model 1

Formula 3.2.1 is meant to be valid for the combined resisting moment of the low stanchions without help from any hog lashing and high stanchions.

$$(3.2.2) \quad M_b = \frac{mg}{n} \cdot \left(a_t \cdot \frac{H}{2} - a_v \cdot \frac{b}{2} \cdot r \right) \cdot \frac{1 - (1 - F)^n}{F} \cdot C$$

Where

H = the height of the stow

b = the width of a stack of packages

r = reduction factor depending on the beginning tilt of the stacks

m = the mass of the stow

$g = 9.81 \text{ m/s}^2$

a_t = transverse acceleration/g

a_v = vertical acceleration/g

μ_i = the internal friction coefficient between the vertical surfaces of adjacent stacks

n = the number of stacks of packages in the stow

$F = \mu_i \cdot \frac{2b}{H}$ is the “internal friction factor”

C = “Interaction coefficient”, $0.7 \leq C \leq 1$

This is a model for determining the required strength in stanchions keeping rigid timber packages with a tendency to tip. The unit is kNm.

In figure 3.2.4 three of the tests with $q = 3$ tiers are displayed as series of points. In the same diagram the model is displayed with lines that have the same colour as the corresponding test data points. The model lines are drawn with the following data:

Number of stacks n	Total mass m (kg)	b (dm)	H (dm)	inner friction μ_i	C	r
4	32.4	0.95	3.9	0.35	1	1
5	40.5	0.95	3.9	0.35	1	1
6	48.6	0.95	3.9	0.35	1	1

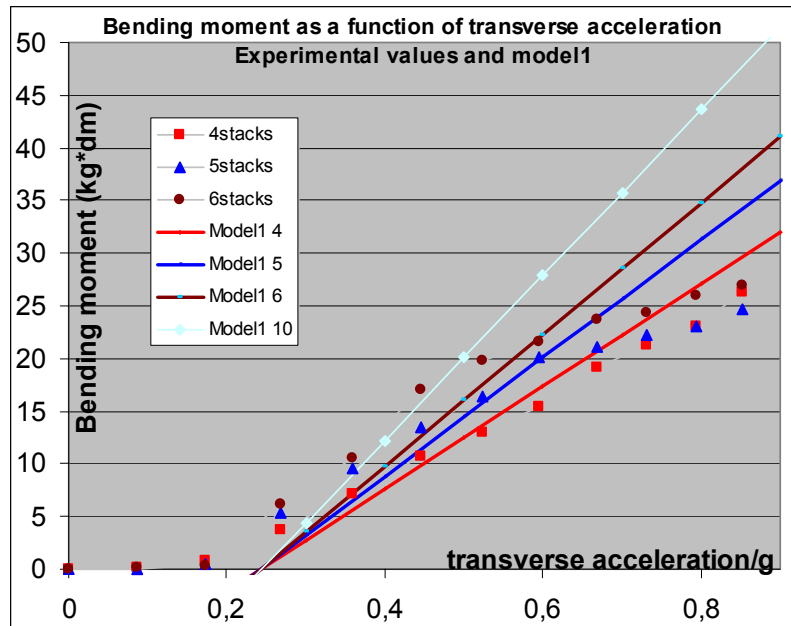


Figure 3.2.5 The model covers the experimental values from about 0.5 g upwards.

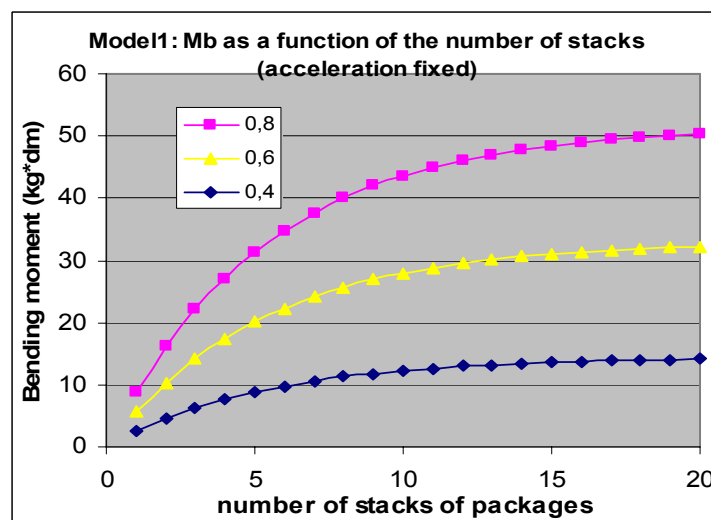


Figure 3.2.6 The increase in the model bending moment declines when more packages are added athwart ships. Each graph shows a fixed acceleration in relation to g.

With $r = 0.5$ and $C = 0.85$ in the model we will get the following results compared to the same test series as above. As can be seen from the left hand diagram of figure 3.2.6 the model has been adjusted so that it covers all the test points. Lowering the value of r raises the level of the model graph, whereas lowering the value of C mainly lowers the slope but also the level.

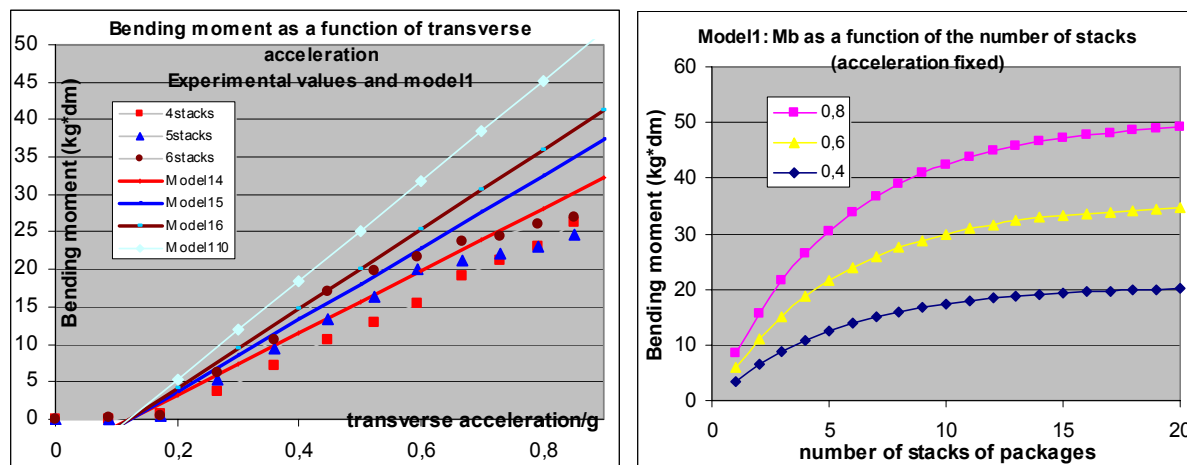


Figure 3.2.7

3.3 Model 2: Firm packages sliding transversally

This approach is close to the imaginary model B sketched in the beginning of this chapter, but with friction added. It is assumed that the packages are firm and are able to slide transversally tier upon tier.

3.3.1 Model tests with transversally sliding packages

In order to make the test as downright as possible 10 mm wooden slats are placed between the tiers so they can slide. Several inclination tests were made starting with 3 tiers and 7-8 packages in each (see figure 3.3.1). Then the number of packages per tier was reduced to 5-6, to 4 and to 2. For each setup the inclination test series was performed three times. The mean values were calculated from the two series that corresponded the best. The results from these first tests can be seen in figure 3.3.3 where the inclination angles are converted into transverse acceleration.



Figure 3.3.1 Wooden slats are placed between the tiers.



Figure 3.3.2 The tiers of firm packages are seen to push on the uprights with their lower corner, the bottom tier not contributing to the total bending moment on the uprights.

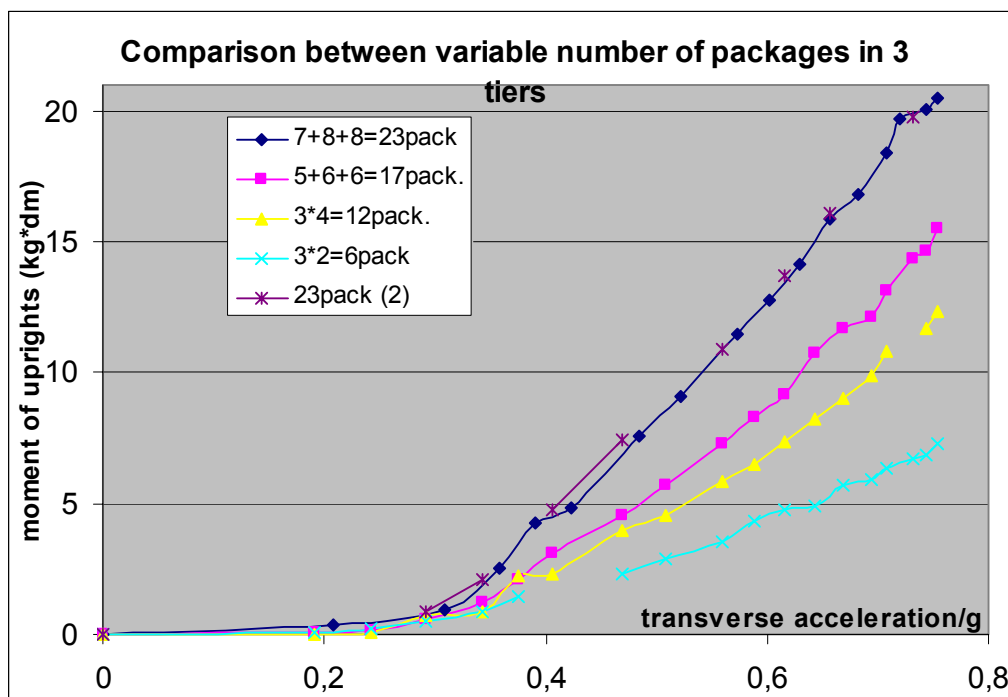


Figure 3.3.3

3.3.2 Force distribution of timber packages against uprights

The uncompressed foam is 10,0 cm thick. At a number of different inclination angles the foam thickness is measured at the bottom corner of each front package on both sides. The mean of the measurements is then subtracted from 10,0 cm and the results are displayed in the diagrams below.

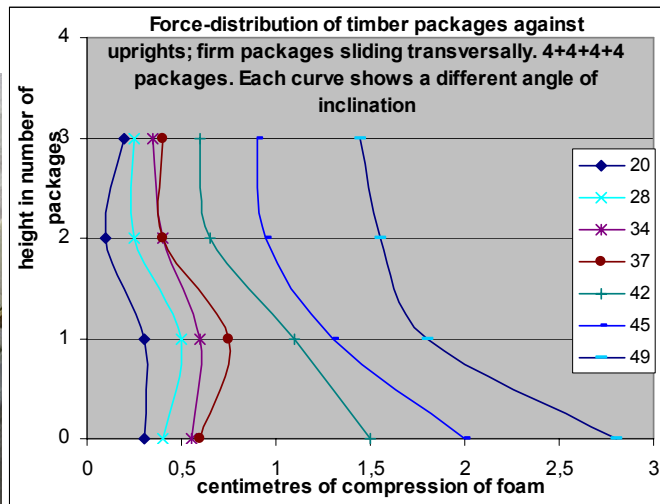


Figure 3.3.4 Force distribution test with four tiers and four packages in each.

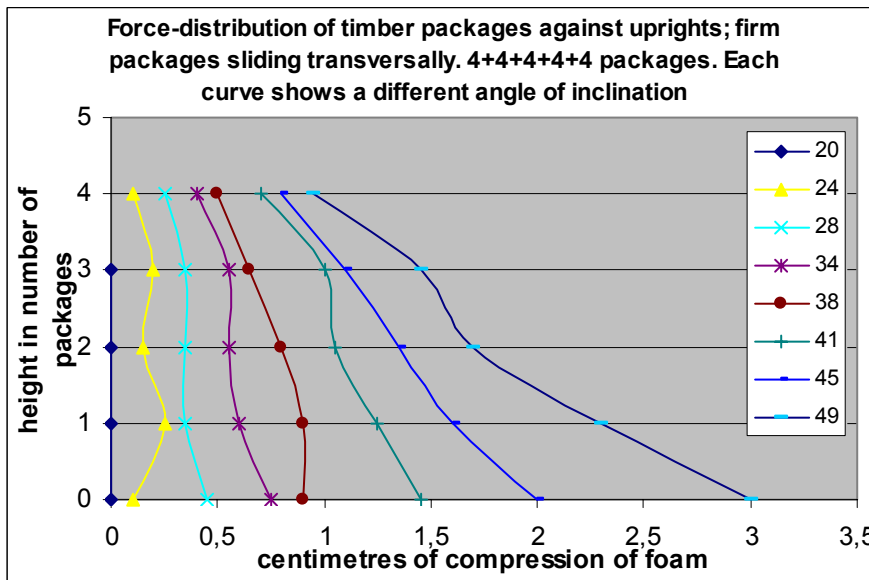


Figure 3.3.5 Force distribution test with five tiers and four packages in each.

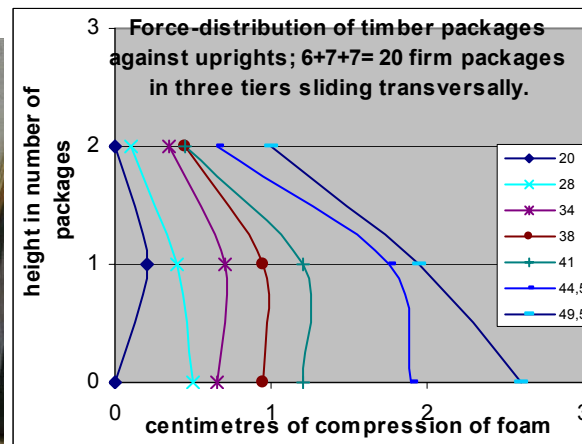


Figure 3.3.6 Force distribution test with three tiers and 6-7 packages in each.

From the force distribution tests can be seen that movement can happen simultaneously in separate contact surfaces, but also in one or two surfaces first and then the others. Towards the end the forces “find their way” down to the bottom.

The centre of the force distributions are calculated using the results from the “foam-tests”.

Number of tiers	Packages/tier	Centre of force distribution in % of H	
		For the entire cargo	For the cargo except the bottom tier
3	4	24 % to 25 %	44 % to 47 %
4	4	27 % to 32 %	44 % to 47 %
5	4	32 % to 35 %	64 % to 67 %
3	6-7	24% to 27 %	38 % to 44 %

Table 3.3

The results in this section ought not to be taken as absolute facts but they give a fair hint about what is happening.

3.3.3 A theoretical approach

It is not evident which tier will slide first. It depends on the friction coefficients of the surfaces and the degree of tightness between the packages. A fair assumption is that the top tier slides first, this is also supported by reference 3 (Karpovich, Karpovich, Voynarovskiy). In fact the transverse acceleration is greater at the top. Nevertheless it is assumed to be the same at all levels for the time being. For simplicity let’s look at a simple example with 3 tiers.

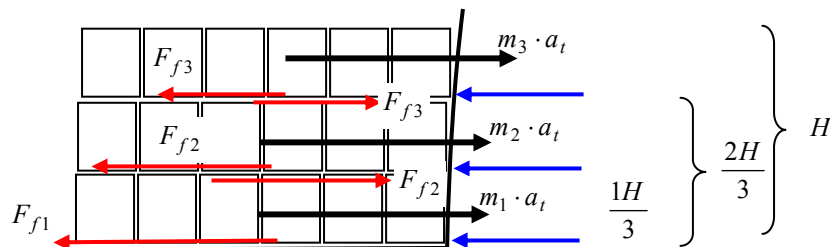


Figure 3.3.7

The top tier moves affected by the acceleration force $m_3 a_t$ and counteracted by the friction force F_{f3} . Then the second tier is pulled by $m_2 a_t$ and F_{f3} and counteracted by F_{f2} . Finally the bottom tier is pulled by $m_1 a_t$ and F_{f2} and counteracted by F_{f1} . The friction forces are then $F_{f1} = \mu_1 \cdot 3m_1 \cdot a_v \cdot g$, $F_{f2} = \mu_2 \cdot 2m_1 \cdot a_v \cdot g$ and $F_{f3} = \mu_2 \cdot m_1 \cdot a_v \cdot g$ (the masses are assumed equal: $m_1 = m_2 = m_3$ and the friction coefficients $\mu_2 = \mu_3$).

As experimentally observed in figure 3.3.2 the front packages in each tier touch the uprights with their low corners. Thus the moment lever for the bottom tier is 0, for the second tier $H/3$ and for the top tier $2H/3$. The resulting bending moment on the uprights would then be:

$$M_b = (m_1 \cdot a_t \cdot g + F_{f2} - F_{f1}) \cdot 0 + (m_2 \cdot a_t \cdot g + F_{f3} - F_{f2}) \cdot \frac{H}{3} + (m_3 \cdot a_t \cdot g - F_{f3}) \cdot \frac{2H}{3}$$

Simplifying and substituting gives:

$$M_b = (m_1 \cdot a_t + \mu_2 \cdot m_1 \cdot a_v - \mu_2 \cdot 2m_1 \cdot a_v) \cdot g \cdot \frac{H}{3} + (m_1 \cdot a_t - \mu_2 \cdot m_1 \cdot a_v) \cdot g \cdot \frac{2H}{3}$$

$$M_b = m_1 \cdot a_t \cdot g \cdot \left(\frac{H}{3} + \frac{2H}{3}\right) + (-\mu_2 \cdot m_1 \cdot a_v \cdot g) \cdot \left(\frac{H}{3} + \frac{2H}{3}\right) = 3 \cdot (m_1 \cdot a_t - \mu_2 \cdot m_1 \cdot a_v) \cdot g \cdot \frac{H}{3}$$

Which results in $M_b = m_{tot} \cdot g \cdot (a_t - \mu_2 \cdot a_v) \cdot \frac{H}{3}$

A similar derivation with q as the number of tiers instead of 3 results in:

$$(3.3.1) \quad M_b = m_{tot} \cdot g \cdot (a_t - \mu_2 \cdot a_v) \cdot \frac{q-1}{2q} \cdot H$$

Which can be interpreted as counting the total mass reduced by that of the bottom tier ($m_{tot} \frac{q-1}{q}$) and putting the lever at half the height (H/2).

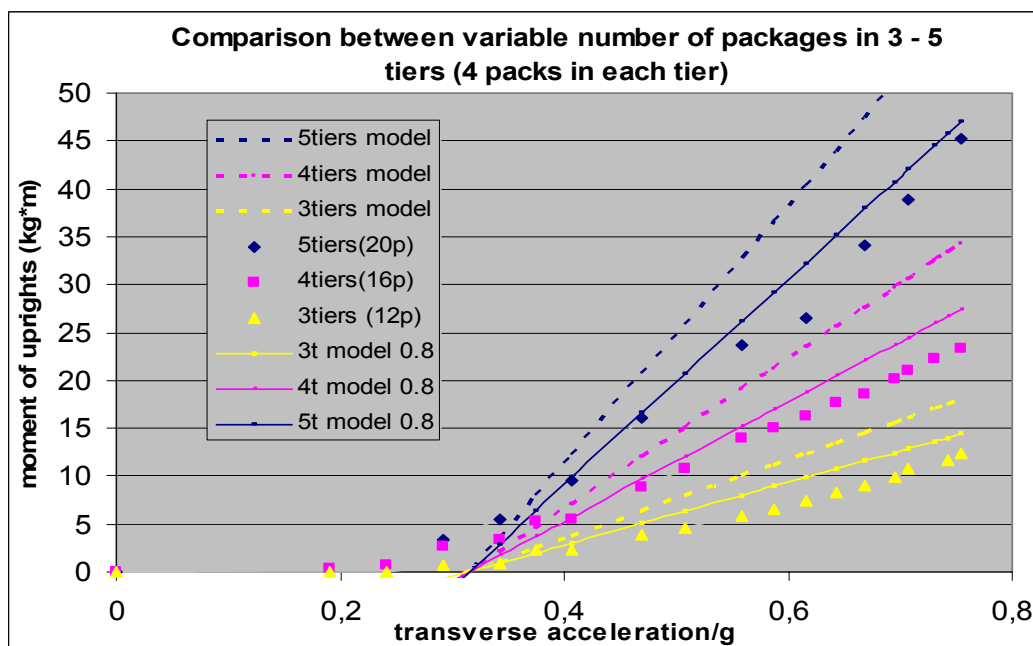


Figure 3.3.8

In figure 3.3.8 is displayed the experimental values and the graphs of the corresponding interpretations with the formula above. The formula clearly gives too high values (The dotted lines). Which means that there are other factors than ordinary friction acting to keep the stow from deforming.

3.3.4 The interaction between individual packages

The tiers are not monolith masses, they consist of a number of separate packages that are standing on various spots of the underlying tier or surface. They move to a certain extent independently. When one or several packages move a little, the others might stay behind and in turn move when the underlying tier starts to move. Some packages from an upper tier can that way be part of a lower tier of packages and contribute to a lowering of the centre of forces. This can be sensed in figures 3.3.4-6. The constellations are infinite and may change in the same stow in changing conditions. This phenomenon is believed to be the additional factor to take into account.

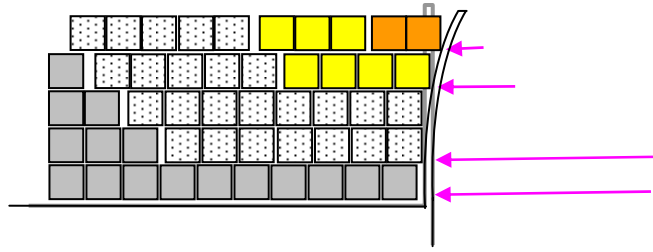


Figure 3.3.9 A possible scenario where sections of the tier act as units and thereby contribute to lowering the centre of the force distribution.

A number of possible constellations have been investigated out of which one simplified is presented below. Assume that half of the packages in the top (third) tier moves and the others stay in place. Instead when part of the second tier moves, half of the remaining top tier follows and finally when the bottom tier moves the remaining packages on top act as an integrated part of it. In this special case there are 3 tiers and a derivation similar to the one starting from figure 3.3.7 with the masses of the three sections $m_1 = m_{tot}/2$, $m_2 = m_{tot}/3$ and $m_3 = m_{tot}/6$ (see figure 3.3.10) will result in the following formula:

$$M_b = m_{tot} (a_t - \mu_2 \cdot g) \cdot \frac{q-1}{2q} \cdot H \cdot \frac{2}{3}$$

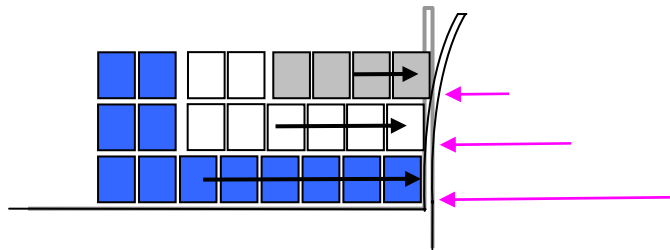


Figure 3.3.10

The formula differs only with a factor 0.67 from formula (3.3.1). With $q = 3$ it means that counting with the entire mass of the stow the lever on the uprights is reduced to about 0.22 H, which is a bit lower than the values suggested in table 3.3. This was an example to illustrate that the effect of “lowering of forces” can be explained in this way. If ever one could know what happens inside the stow the effect can be modelled by multiplying an “interaction coefficient” C to the formula. In general $0.7 \leq C \leq 1$. The wider and the lower the stow, the lower C could be set (compare with the results from section 3.3.2). To retain a security margin C should be set to 1.

3.3.5 The formula for transversally sliding packages: Model 2

With the background from the experiments and the above discussion the final formula for the sliding packages is obtained.

$$(3.3.3) \quad M_b = m \cdot g \cdot (a_t - \mu_2 \cdot a_v) \cdot \frac{q-1}{2q} \cdot H \cdot C$$

Where

H = the height of the stow

m = the mass of the stow

$g = 9.81 \text{ m/s}^2$

a_t = transverse acceleration/g

a_v = vertical acceleration/g

μ_2 = the friction coefficient between the horizontal surfaces between the tiers

q = the number of tiers

C = the interaction coefficient ($0.7 \leq C \leq 1.$)

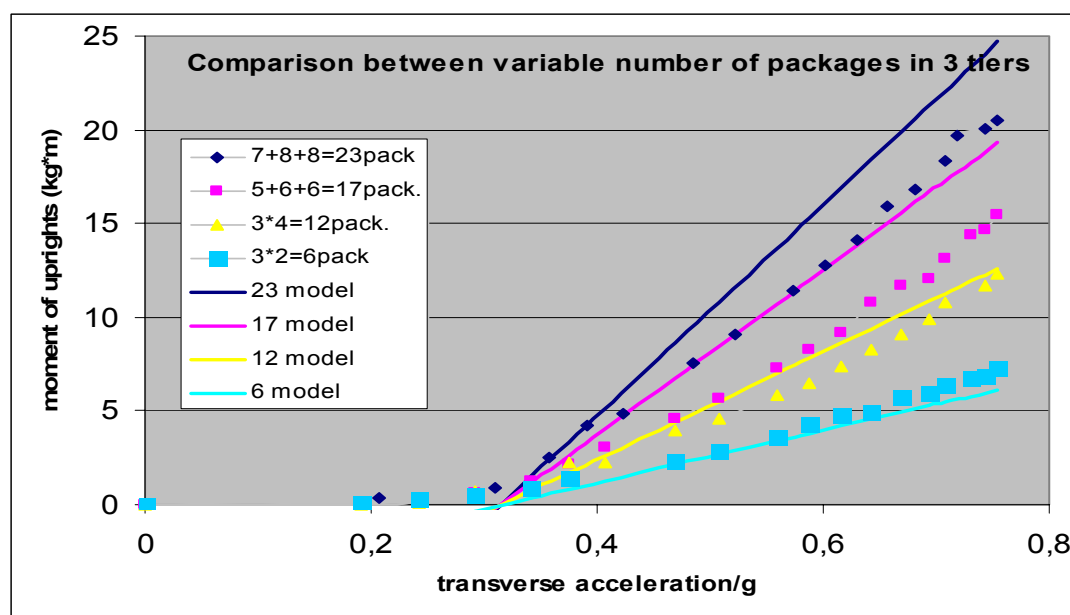


Figure 3.3.11 The formula is applied to a number of test series with a variable number of horizontally sliding packages in three tiers (figure 3.3.1 shows one of them). The value of C is put to 0.7. The other values are listed in the table below.

Number of packs/tier	q	Total mass m (kg)	H (dm)	friction between the tiers μ_2	C
7-8	3	61.7	3.9	$0.7 * 0.45 = 0.3$	0.7
5-6	3	48.5	3.9	$0.7 * 0.45 = 0.3$	0.7
4	3	31.5	3.9	$0.7 * 0.45 = 0.3$	0.7
2	3	15.3	3.9	$0.7 * 0.45 = 0.3$	0.7

3.4 Model 3: Counting with non-firm timber packages

3.4.1 Deformed packages and collapsed packages

The load on top of a package of sawn timber can with sufficient force either slide on top of the package or deform it. If the load presses sufficiently and there is a sideways movement the package can rack, that is become like a parallelogram (figure 3.4.2). Or it can even collapse (figure 3.4.1). The capacity of the package to resist this is called “racking strength” RS, defined below. If the friction force between the load and the package is greater than the RS and the sideways force is in the vicinity of or greater than the RS, then deformation to some extent will occur.



Figure 3.4.1 a) Sling lifting damaging packages b) collapsed, “barrelled” package

The racking strength was defined in the report from Sundsvall (Reference 1, section 6.3, Andersson, Sökjer-Petersen) as a result of practical trials: *The racking strength, RS, of a timber package is taken as the force that produces a deformation at the top of the package of 100 mm or 10% of the package’s width.* Obviously RS can be taken as the capacity for the package to resist such a deformation. As the strappings are often nowadays of elastic material, soon after – or even before - such a deformation the package can collapse as mentioned before. “Thanks to” the elasticity of the strappings the content mostly still stays together but in a “barrelled” form. But packages collapse rather because of poor stowage procedures or even when lifting with sling (Figure 3.4.1 a). In the following the packages are assumed in certain conditions to deform but not to collapse. The model packages in this investigation were thoroughly examined in respect to their capacity to rack.

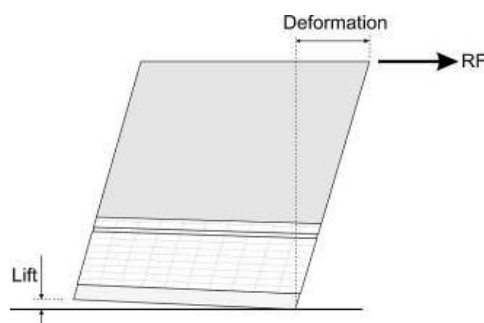


Figure 3.4.2 Timber package deformed due to vertical pressure and simultaneous transversal force.

3.4.2 Determination of internal friction of packages with poor form stability

A number of “y-type” packages were placed on the test surface with blockings between them (figure 3.4.3) The angles when the first and the last package to rack were noted. In this experiment each package was tied with three rubber bands in a simple loop. The result is in table 3.3 below. When the packages are tied with double looped rubber bands only a few of them will rack before the inclination becomes so steep that they will fall on top of each other.



Figure 3.4.3

Rackable packages on an inclined plane; blockings between each package. The inclination angle when the packages rack is noted				
first	middle	last	average (degrees)	
26	26	26	26,00	
23	24,5	28	25,17	
23,5	28,8	32,5	28,27	
25,5	26,5	31	27,67	
21,5	24	30	25,17	
average			26,28	
tan(26,28°)		= μ =	0,49	

Table 3.3 Determination of the "internal friction factor".

3.4.3 Determination of the racking strength of the packages

Seven numbered (y1, y2, y3, y4, y6, y7 and "X") model packages were tested in a similar way as some real full scale packages in the tests in Sundsvall February 2008. The packages were tied with three one-loop rubber bands.

- Pack X is a "look-alike" package with "boards" of 15mm*10mm.
- The other six packages are built up of wooden boards and sheets of masonite.
- Dimensions (L*B*H) 4dm*1,0 dm* 1,2 dm for all.
- Weight: ranging from 2,7 to 3,15 kg, except for pack X that weights 1,9 kg.

Racking tests on model timber packages		5.2.2009					
RS = Racking strength		1,2	dm	β =	20,0	degr.	
					0,3488	rad	

Figure 3.4.4



a)



b)



c)



d)



e)

Figure 3.4.5 a, b) Racking tests with package named X. c) Testing package nr y1. d) Racking package nr y7. e) Distance to firm upright measured with ruler sliding on top of the package. f, g) Corresponding full scale tests in Sundsvall February 2008.



f)



g)

Pack X weight 1,9 kg b = 20,4					
height 1,23 dm					
F	dist	deform.	F	dist	deform.
0,00	30	0	0	31	0
0,32	29	1	0,43	30	1
0,48	28	2	0,63	29	2
0,55	27	3	0,65	28	3
0,72	25	5	0,75	27	4
0,79	23	7	0,78	26	5
0,85	23	7	0,88	24	7
0,88	22	8	0,96	22	9
0,95	21	9	1,1	17	14
1,02	20	10	1,25	15	16
1,05	19	11	0	18	13
0,00	21	9			
F(20mmr 1,02 kg		F = 0,99 kg			
RS = 0,96 kg		RS = 0,93 kg			

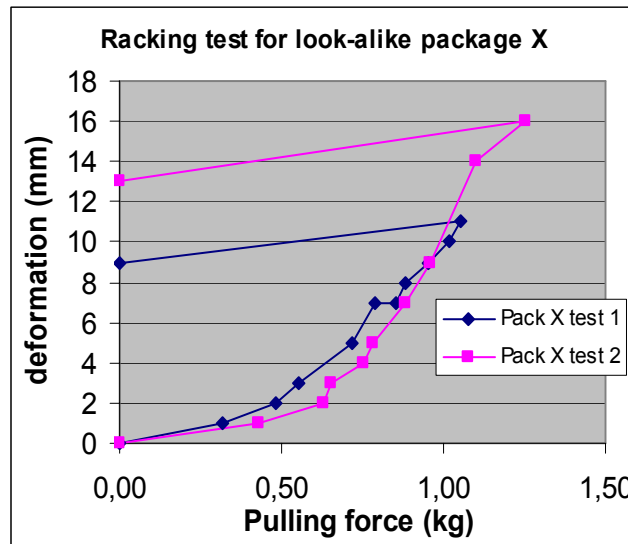


Table 3.4 Racking tests for package X with single loop rubber bands. The graphs are smoother than the ones for the y-packages.

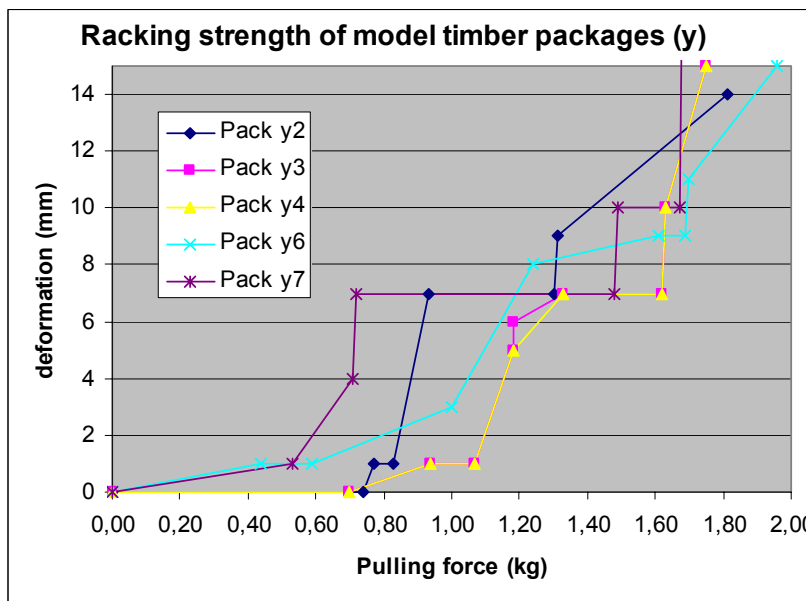


Table 3.5 Average racking strength for the "y-type" packages with single loop rubber bands

RS	
Pack y1	1,20
	1,39 4,29
Pack y2	1,32
Pack y3	1,38
Pack y4	1,53
Pack y6	4,59
Pack y7	1,39
Average	1,41 kg

Figure 3.4.6 Diagram showing deformation of packages as a function of the racking force. The graphs show the jerky and irregular behaviour of y-packages

The packages are tied with two of the rubber bands doubled in the next test. Only the results are given. From the diagram in figure 3.4.7 can be seen that the jerkyness prevails.

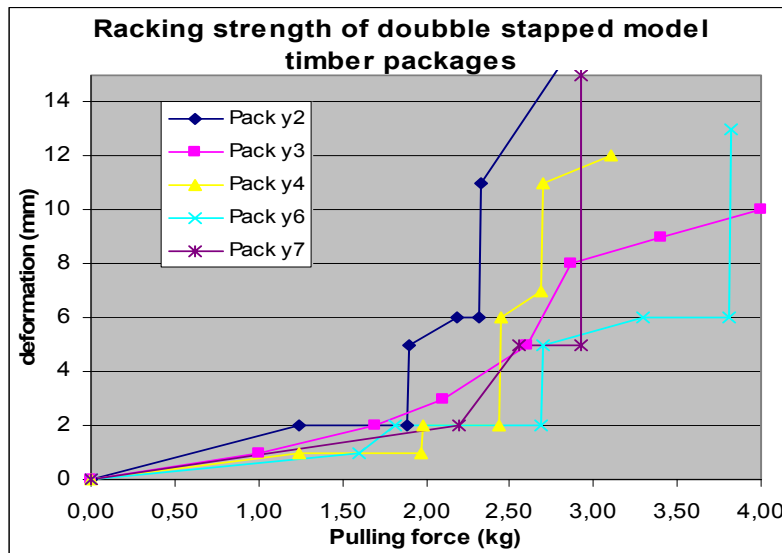


Table 3.6 Average racking strength for the “y-type” packages with double loop rubber bands.

RS	
Pack y1	2,25
Pack y2	2,18
Pack y3	3,74
Pack y4	2,53
Pack y6	3,58
Pack y7	2,74
Average	2,76 kg

Figure 3.4.7 Diagram showing deformation resulting from racking force. The graphs show the jerky and irregular behaviour.

The calculated RS is 0,95 kg for X (table 3.4) and about 1,4 kg in average for the others, the y-packages (table 3.5) when the packages are tied with three single loop rubber bands. When two of the rubber bands are doubled the calculated RS is 1,87 kg for X and about 2,76 kg in average for the others,

As a whole the y-type packages with masonite sheets move in a jerky and irregular way. The experiments made with sets of only y-packages are not very reliable. In the next section an improvement was made.

3.4.4 Racking strength as a function of the super positioned load

A series of new “x-model” packages were put together in the spring months of 2009. The packages numbered x1...x8 are constructed in exactly the same way with model “boards” measuring 5 mm * 15 mm * 400 mm, 9 stickers of 1 mm plywood in three levels, three beams at the bottom and tree on top and strapped with rubber bands. The packages numbered x9 to x14 are assembled in the same way but consist of thicker and in parts rougher model boards. The RS-values were determined in the same way as in the previous section and the results are displayed in figure 3.4.9. The “x-packages behave as the ones in the full scale tests in Sundsvall. Only the pulling force when the package has racked 10 mm is noted in each test.

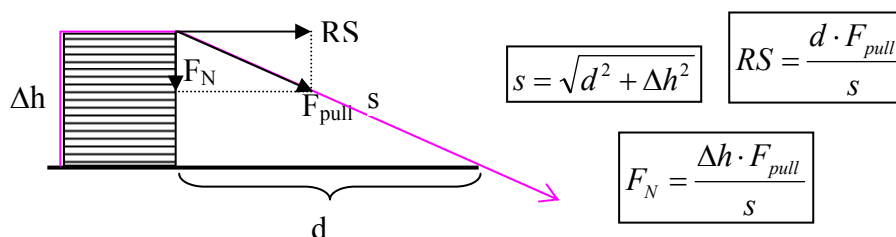


Figure 3.4.8

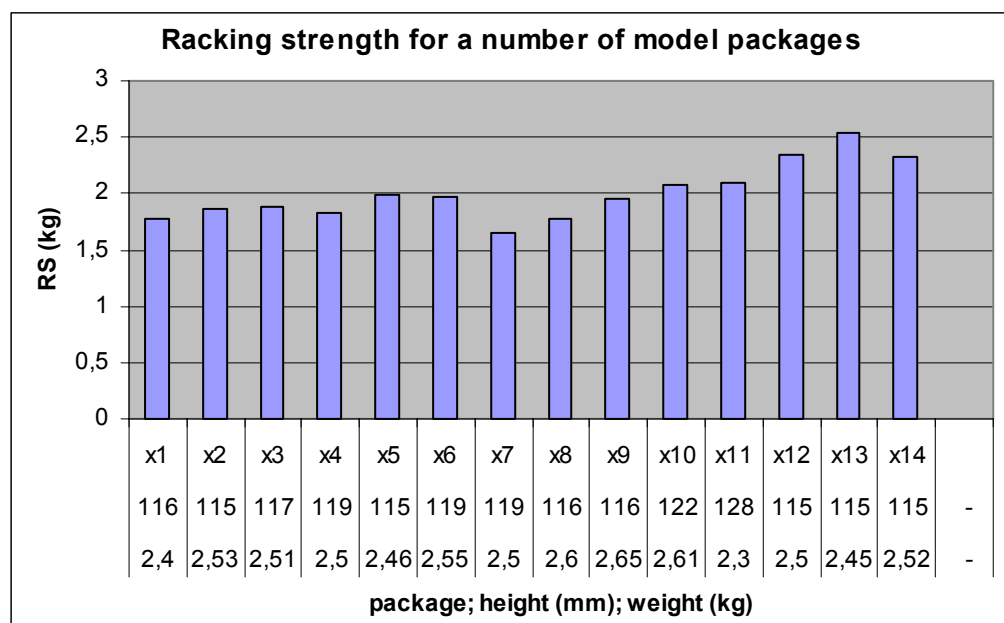


Figure 3.4.9



Figure 3.4.10 determination of racking strength as a function of added super positioned weight.

The experiment proceeds then by successively adding more weight on top of the packages and making the same measurements (see figure 3.4.10). As an example the results from package number x6 are displayed in table 3.8. The results (in bold type) are plotted together with the corresponding results from the other tested packages in figure 3.4.11. The graph for each package is shown to be almost linear. The packages x1 to x11 that are similar in composition have graphs with a slope between 0.30 and 0.40 which is about the value of the static friction coefficient of two surfaces of fine sawn or planed wood. In fact the slope of the line is the ratio between the increase in the racking force and the increase in the weight on top, which is the definition of a friction coefficient. So the slope of the line equals the inner friction coefficient of the package. The constant in the equation is then roughly the initial racking force RS. Thereby the following relation can be set up:

$$(3.4.1) \quad RS_q = RS_l + \mu_i * (q-1) * m_p$$

Where

q is the number of packages in the stack including the bottom one,

RS_q is the racking strength of the bottom package with q packages in the stack,
 RS_I is the initial racking strength of the package without any other ones on top of it,
 μ_i is the inner friction coefficient of the bottom package, and
 m_p is the mass of one package.

pack	x6						height (Δh) =	119 mm	Weight 2,55 kg
number of super positioned packages:	1	2	3	4	5	6			
additional superpos.weight	2,46	2,5	2,5	2,51	2,53	2,6		kg	
Tot.sup.p.weightht	0	2,46	4,96	7,46	9,97	12,5		15,1 kg	
pulling force (kg) when 10mm ls passed	2,25	3,31	4,09	5,25	5,89	6,28	7,46		
	2,07	3,36	4,08	5,08	5,91	6,4	6,93		
	2,13	3,24	4,22	5,05	5,51	6,2	6,73		
	2,03	3,24	4,07	5,02	5,49	6,07	7,09		
	2,08	3,16	4,02	5,05	5,9	6,07	7,24		
central mean	2,093	3,263	4,08	5,06	5,767	6,183	7,087	kg	
line length (s)	353,6	353,6	353,6	353,6	353,6	353,6	353,6	mm	
RS =	1,971	3,073	3,842	4,765	5,43	5,823	6,673	kg	
FN =	0,704	1,098	1,373	1,703	1,941	2,081	2,385	kg	

Table 3.8 The test results for the package x6 given as an example. The results for all x-packages are displayed in figure 3.4.11.

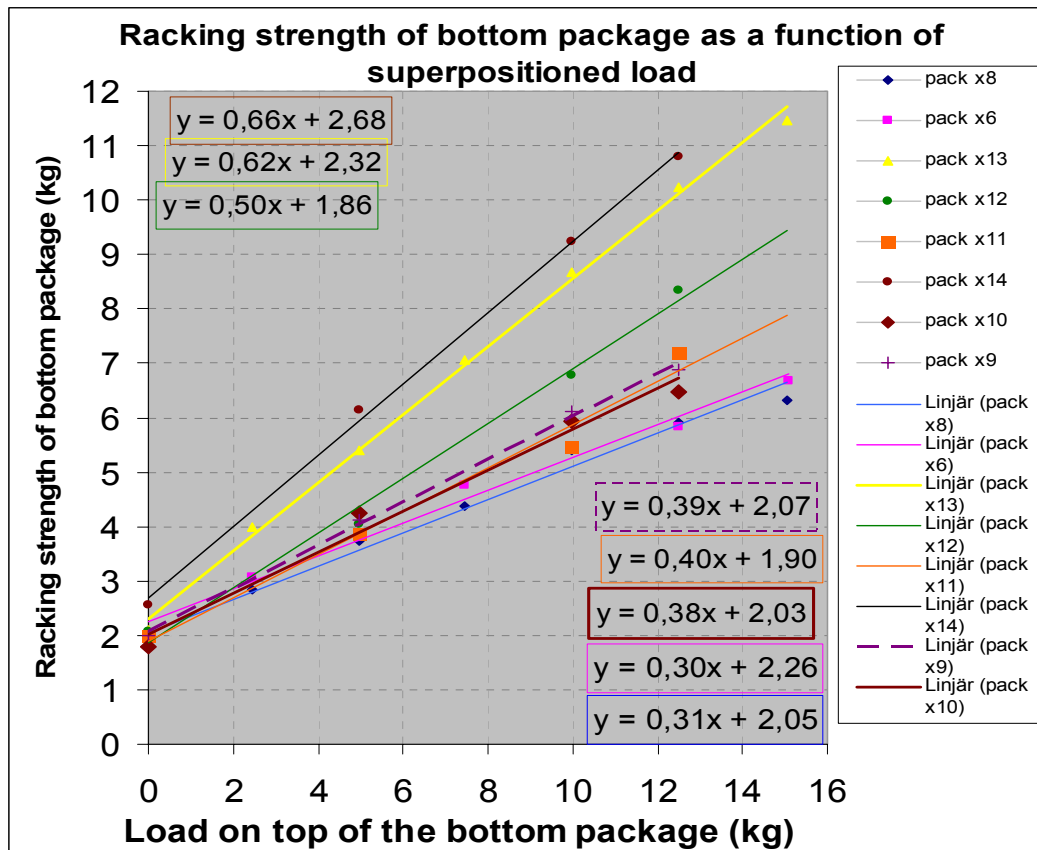


Figure 3.4.11 The graphs of the most realistic model packages x1 to x11 stay very close (the bottom set of five equations).

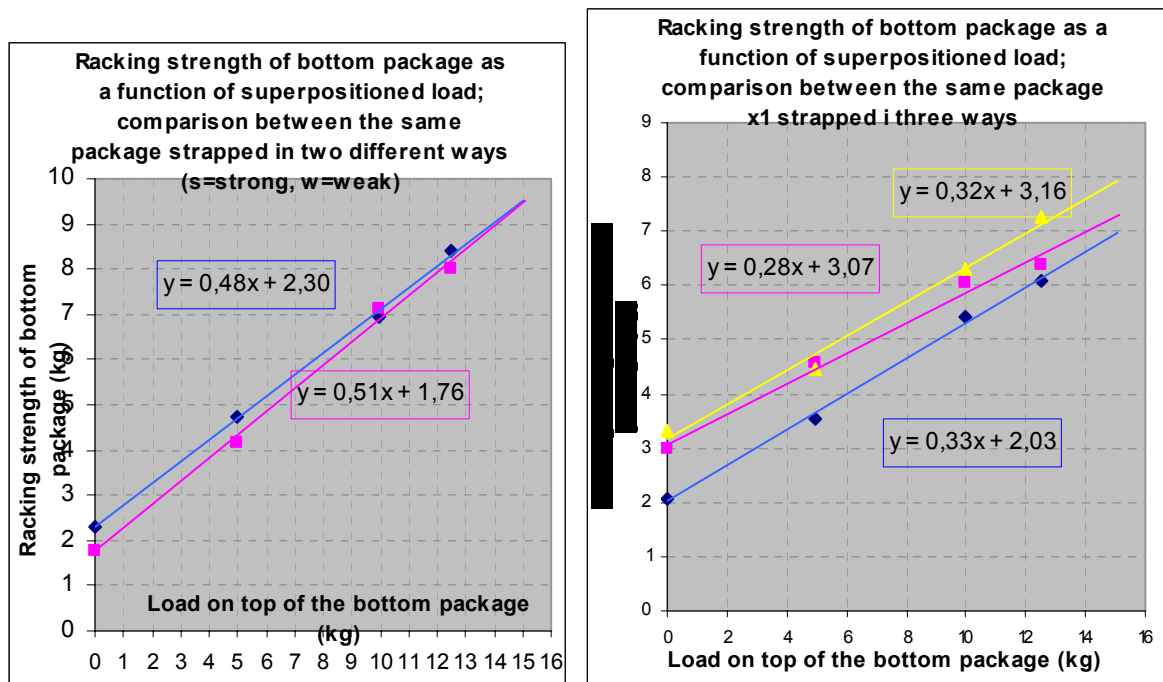
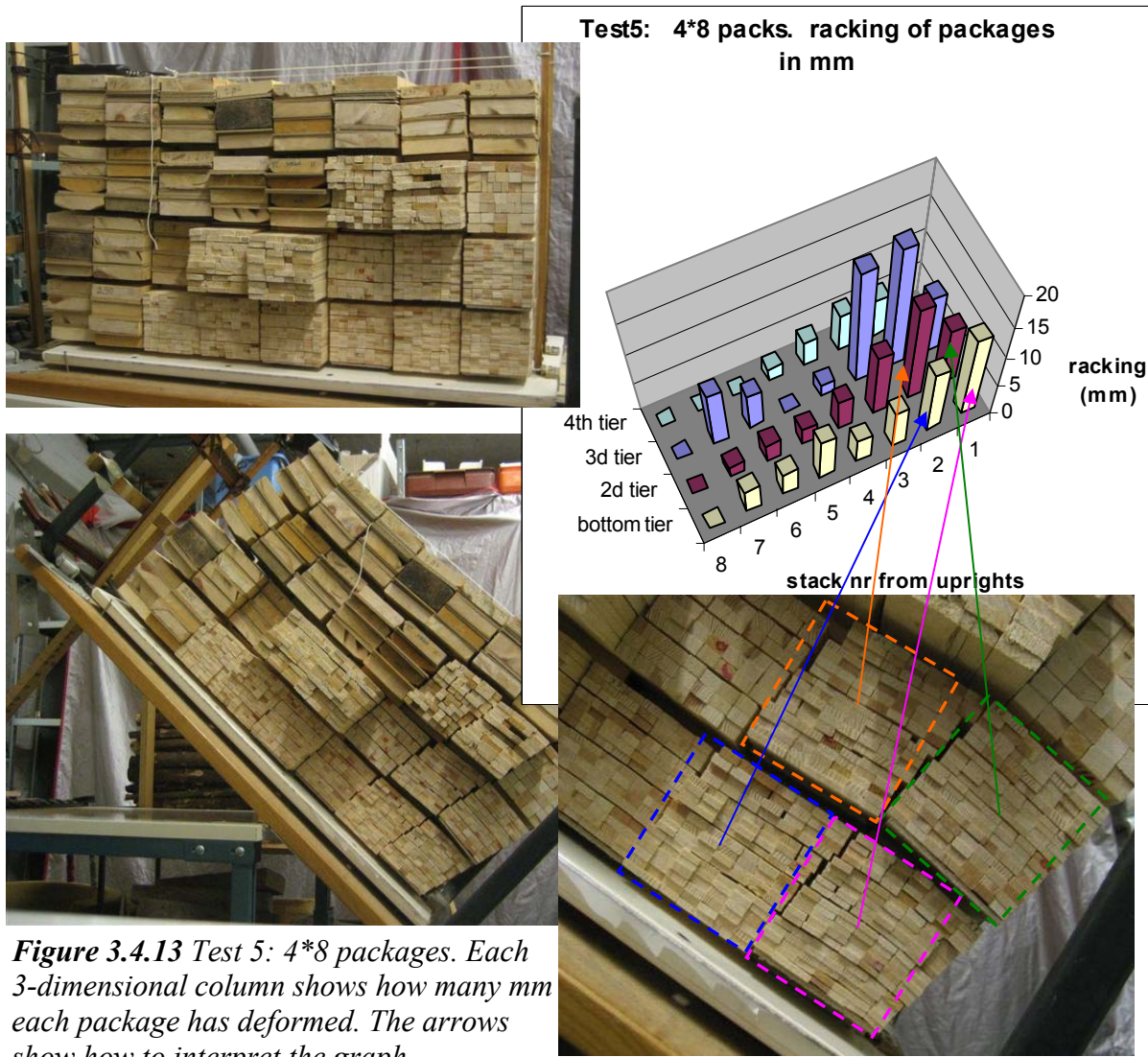


Figure 3.4.12 a) Graphs of y-type package strapped in two different ways converge as the weight increases. **b)** Graphs of x-type package strapped in three different ways converge or keep the same slope.

3.4.5 Deformation of timber packages as a function of their position in the stow

A number of inclination tests were performed with variable numbers of tiers and stacks with potentially deformable model timber packages. The deformation of the individual packages in the stow was measured and mapped. Some of the results are displayed below. As can be seen from the pictures and the graphs the packages in the “downward corner” deform in general the most. This seems like a natural thing when you look at the pictures that the rest of the stow presses almost diagonally on top of the packages in the downward corner. When a strong acceleration force acts transversally on a deck cargo the resulting force also aims diagonally downwards. The pressure bends the low uprights outwards. There are irregularities in the graph due to differences in package composition, size, strapping and especially due to occasional void spaces in the stow. Nevertheless a couple of general conclusions can be drawn from these tests: 1. The packages that deform the most are in the stacks closest to the uprights. 2. The packages in the uppermost tier deform the least. 3. The two or three stacks (roughly one third of the stow) most behind tip (lean) against the rest of the stow rather than just deform.

As a conclusion approximately a trapezoidal portion of the stow closest to the uprights contains the packages that are the most liable to deform, i.e. their ability to resist deformation is decisive for the form stability of the entire stow. About one quarter of the packages can be said to use their racking strength RS to resist the deformation of the stow. The fact that the back third of the packages do not act as an integrated part of the stow - they merely lean against the back of it - means that they do not fully contribute to the effective weight of the stow against the uprights. See figures 3.4.13, 14 and 15.



*Figure 3.4.13 Test 5: 4*8 packages. Each 3-dimensional column shows how many mm each package has deformed. The arrows show how to interpret the graph.*

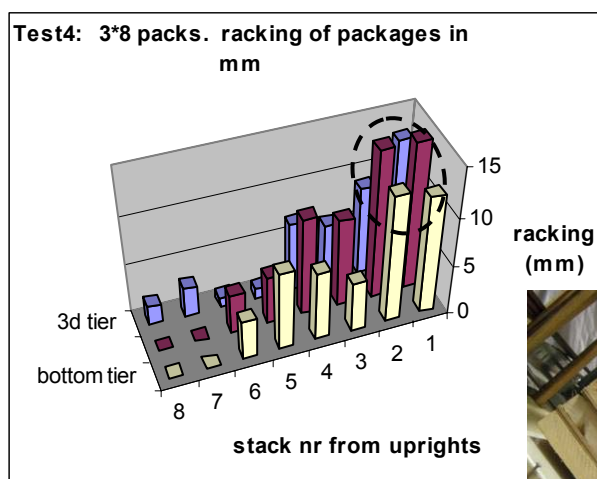


Figure 3.4.14 shows that roughly one quarter of the packages "use" their Racking strength (they deform more than 10 mm). The back stacks are seen to tip, rather than deform.

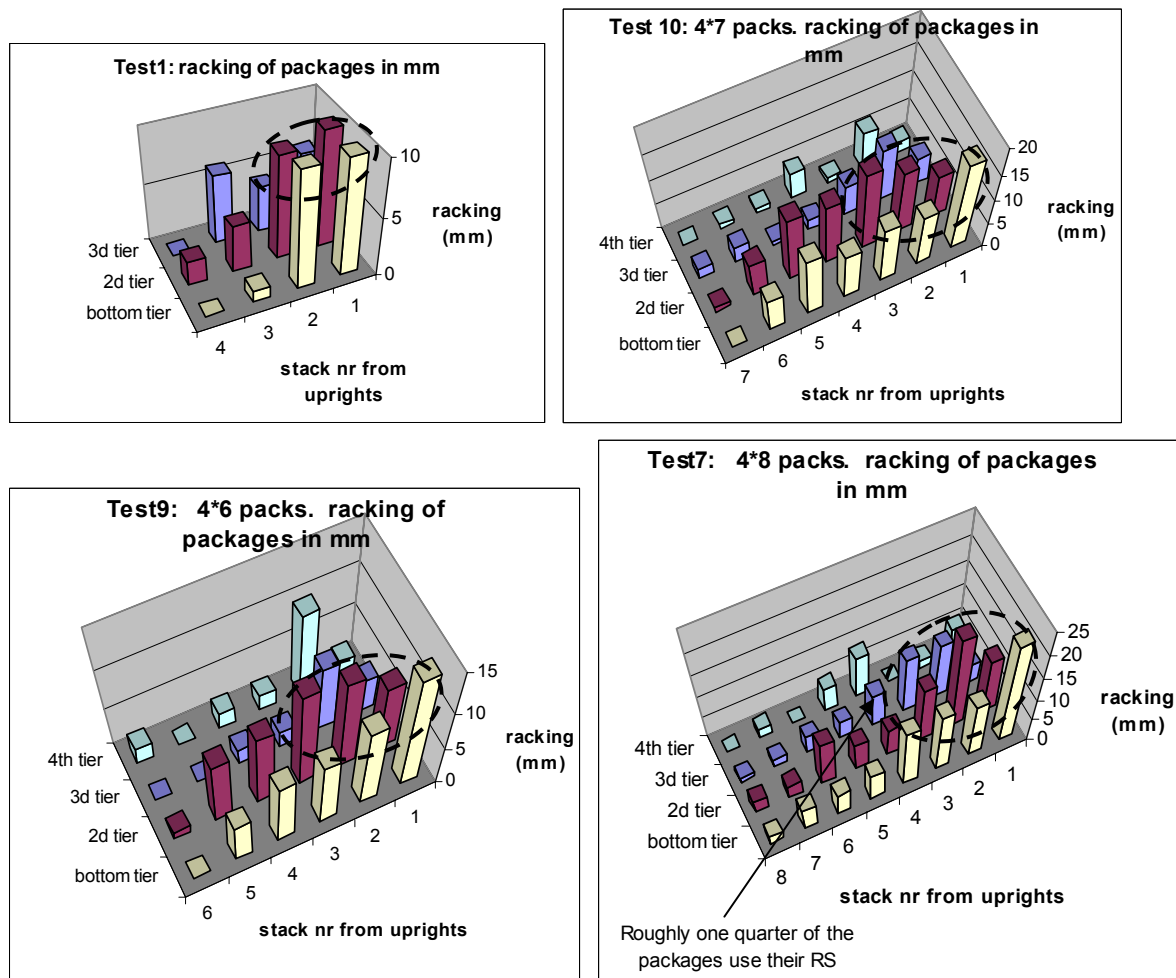


Figure 3.4.15 Measured deformation of the packages from four more tests. Roughly one quarter of the packages are deformed 10 mm or more.

3.4.6 Inclination tests with a variable number of stacks of deformable packages

A great number of inclination tests were made with potentially deformable model timber packages. In addition to the results presented in the draft to this report the 17th of February 2009, tests with the true x-type model packages were made in many different constellations. The dynamometer readings (kg) were noted for a number of angles. The moments were then calculated by multiplying the readings with the height h (in dm) where the strings to the dynamometers were attached. Pictures of some of those can be seen in the previous subsection. The number of tiers were varied from 3 to 4 and the number of stacks from 4 to 8. The x-type packages that behave realistically were first placed in the bottom tier and then in the front stacks closest to the low uprights. In the previous subsection the implications from that were discussed. At the end of next subsection the results from the tests are displayed in a number of diagrams together with the graphs of the model formula.

3.4.7 A theoretical approach on the “soft” packages: Model 3

As figures 3.4.13-15 show only the bottom and the most advanced packages will be liable to deform or in other words to use their racking strength efficiently to resist racking of the entire stow. Thereby it is assumed that the top tier is not in any decisive manner pressing against the uprights because it does not rack and thus does not reach the (bent) uprights, but the top tier will contribute with its weight. Likewise the stacks behind do not rack and only contribute with their weight. So from these observations and assumptions it is deduced that the impact on the stanchions is the height of the cargo minus the height of the top tier. The centre of impact is thus at half of that height:

$$\frac{(q-1) \cdot H}{q} \cdot \frac{1}{2},$$

where q is the number of tiers and H the height of the cargo. If the cargo is three packages high ($q = 3$), then the centre of impact is at $H/3$. In figure 3.4.16 below $q = 4$, so the centre of impact is calculated to $0.38 H$.

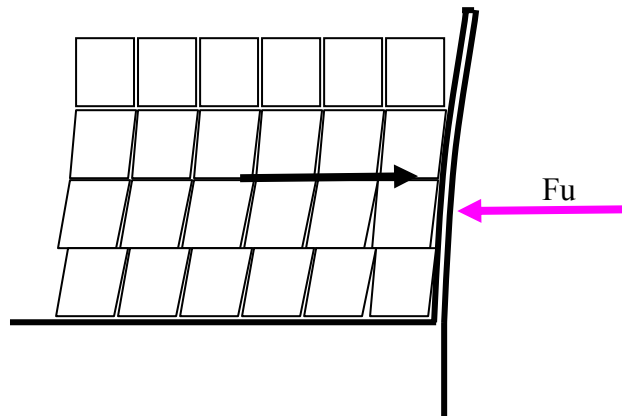


Figure 3.4.16

Furthermore, as mentioned above only a reduced number of packages will effectively resist the deformation of the stow and thereby resist the acceleration force against the uprights with their racking strength (RS). From section 3.4.5 it is seen that about a quarter of the packages deform 10 mm or more. From this is deduced that the resulting force resisting deformation of the entire stow is equal to the sum of the RS of about a quarter of the packages. If the number of stacks is n , and the number of tiers q , then that reduced number of contributing packages would be $f_{RS} \cdot q \cdot n$ where f_{RS} is suggested to be equal to 0.25. The resulting force against the uprights is then $m_{tot} \cdot a_t \cdot g - 0.25 \cdot q \cdot n \cdot RS$. And the moment would then be:

$$(3.4.2) \quad M_b = (m_{tot} \cdot a_t \cdot g - f_{RS} \cdot q \cdot n \cdot RS) \cdot \frac{(q-1)}{2q} \cdot H.$$

A numerical example: The number of packages in a stow is $n \cdot q = 12 \cdot 6 = 72$. The total mass is $m_{tot} = 72 \cdot 2.5 \text{ ton} = 180 \text{ ton}$. The height is $H = 7.0 \text{ m}$ and the racking strength $RS = 1.5 \text{ ton}$. The “RS fraction factor” f_{RS} is 0.25. Then the required moment as a function of the transversal acceleration would be:

$$M_b = (180 \cdot a_t - 0.25 \cdot 12 \cdot 6 \cdot 1.5) \cdot \frac{(6-1)}{2 \cdot 6} \cdot 7 = 525 a_t - 79.$$

The model is linear with respect to the transverse acceleration. The model graph is plotted in the diagrams below.

Comparing this model (with $f_{RS} = 0.25$) to the experimental values it appears that the model graph has the same slope and it fits perfectly the experimental values from the tests with $n = 8$ stacks of packages, see figures 3.4.19-20.

How well does the model fit the experimental values with a differing number of stacks n ? The total mass $m_{tot} = q \cdot n \cdot m_p$, where m_p is the average mass of one package. Then formula (3.4.2) becomes

$$M_b = (q \cdot n \cdot m_p \cdot a_t \cdot g - f_{RS} \cdot q \cdot n \cdot RS) \cdot \frac{(q-1)}{2q} \cdot H = n \cdot (m_p \cdot a_t \cdot g - f_{RS} \cdot RS) \cdot \frac{(q-1)}{2} \cdot H$$

Which means that the bending moment M_b is proportional to the number of stacks n , with the other variables fixed. In that respect the model does not fit all the experimental values exactly as long as the factor f_{RS} is kept constant. In fact the increase in M_b for the experimental values becomes a little bit smaller with every added stack. That means that - with f_{RS} fixed at 0.25 - when increasing the number of stacks from $n = 8$ the model will give a little growing security margin, which is not undesirable. On the other hand when the number of stacks grows smaller than 8 the model would at some stage start to give too small values of M_b . But that should not be a problem either because most deck cargoes tend to be wider. And in fact this seems to start happening only for n equal or smaller than 5 in figure 3.4.19.

On the other hand the model doesn't fit as well the old test material from January 2009 with only y-type packages. Those packages do not behave in a "natural" way. The sheets of masonite in the y-packages act in a jerky way and slide "all the way" when they start. The test series with y-packages with $RS = 1.4$ kg are displayed in figure 3.4.18 the model suits the material for 7 stacks almost acceptably, but it is too low for 6 stacks and even lower for 5 stacks. But that means again that increasing the number from 7 stacks the model will give a fit with a growing security margin. Figure 3.4.17 displays the first tests with deformable y-packages. The model fits acceptably.

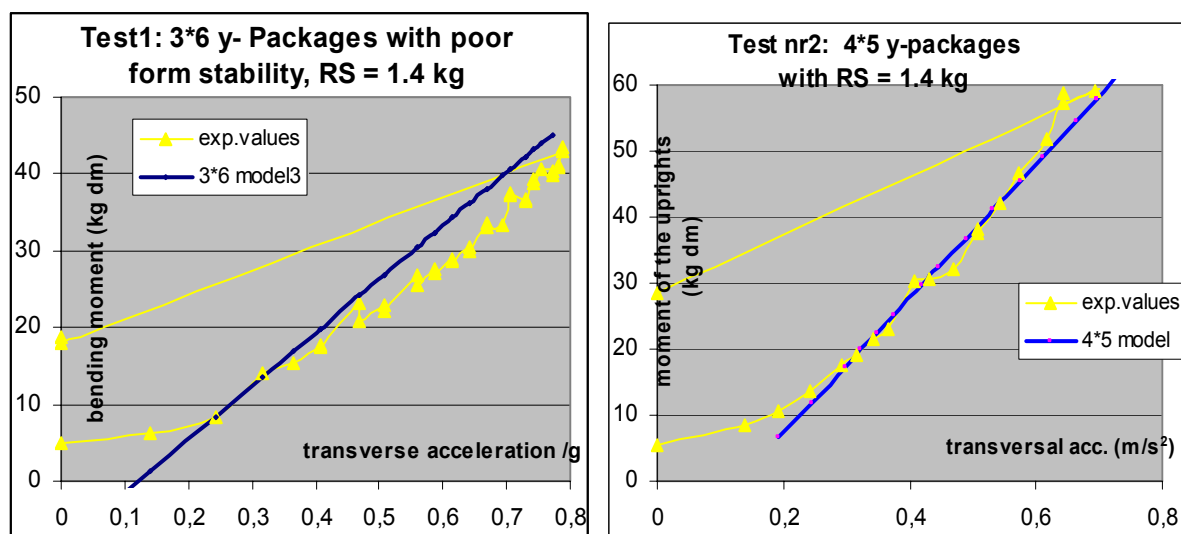


Figure 3.4.17 The first two tests with loose y-packages and model 3.

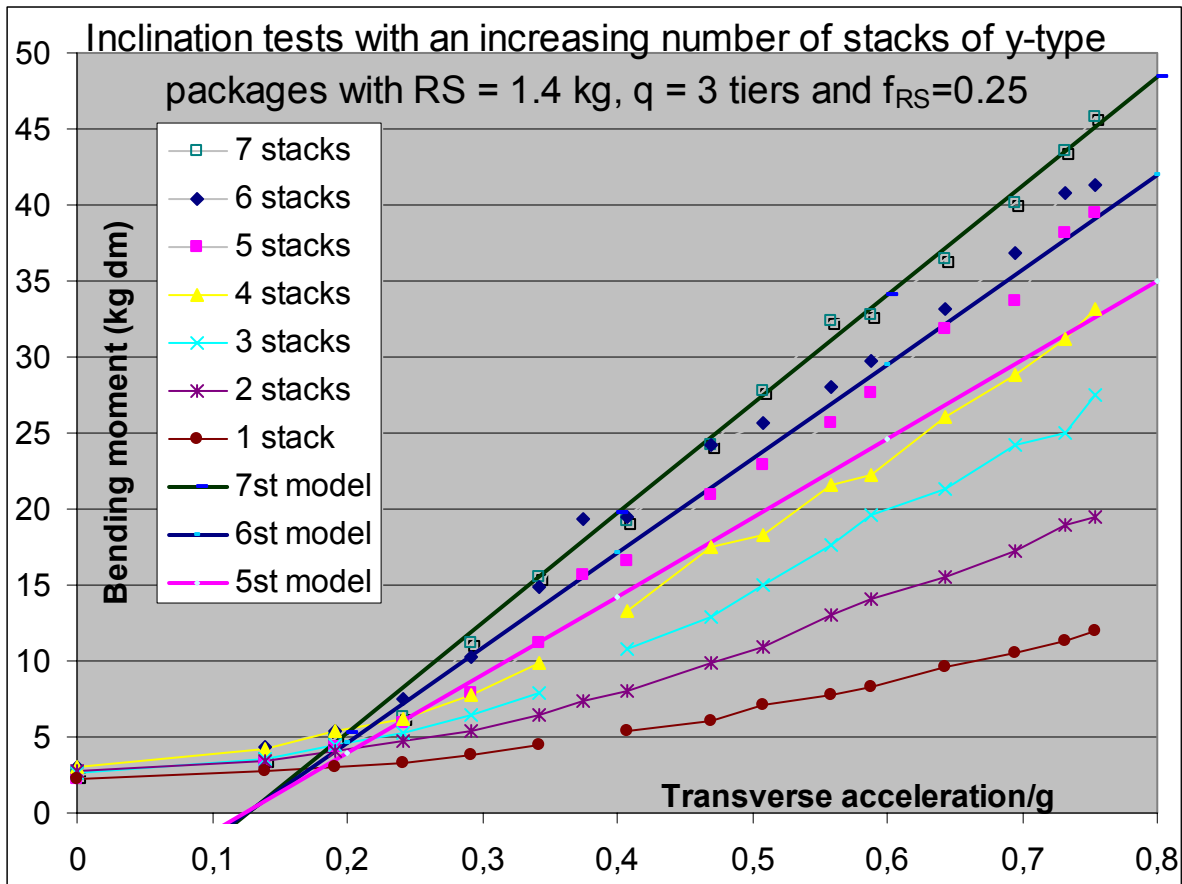


Figure 3.4.11 Graph of the experimental results with proposed theoretical formula plotted

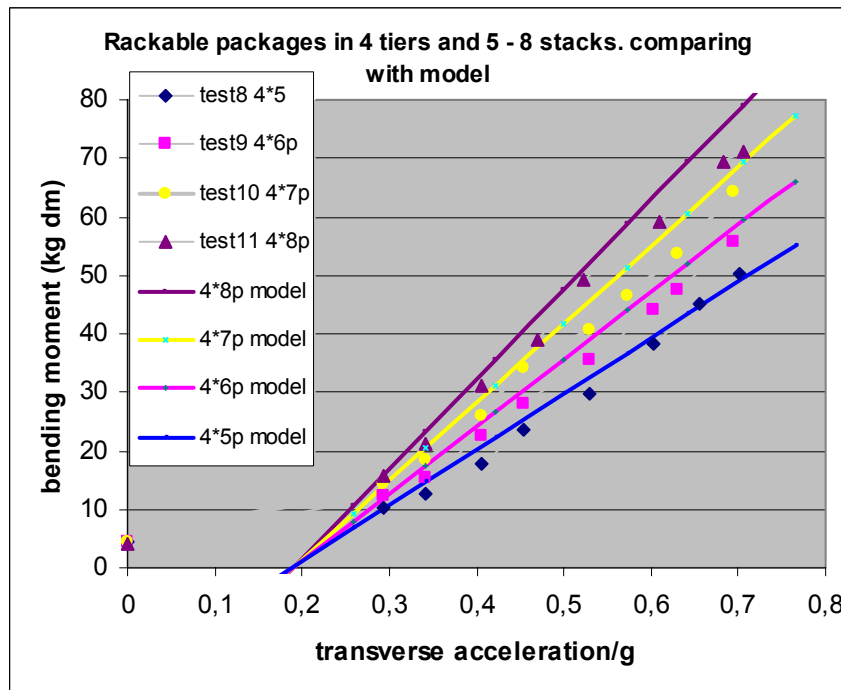


Figure 3.4.12 Tests made with mainly x-type packages with RS about $2,0 \text{ kg}$.

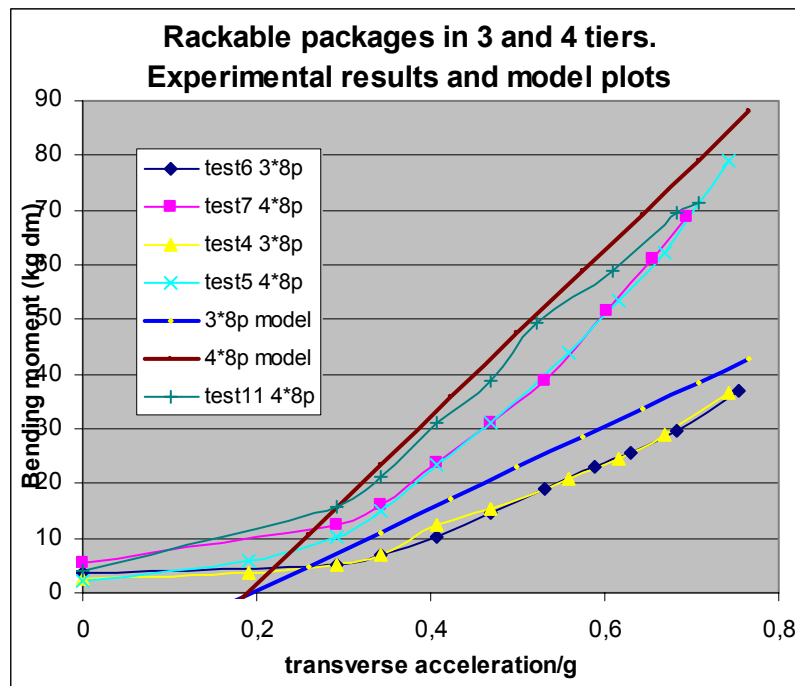


Figure 3.4.13 Tests made with mainly x-type packages with RS about 2,0 kg.

3.4.8 The formula for deformable packages

The above testing and discussion have shown that formula (3.4.2) fulfils the expectations. The only remark would be that f_{RS} could be set a little lower in order to add a security margin if such a margin should be required.

$$(3.4.2) \quad M_b = (m \cdot a_t \cdot g - f_{RS} \cdot q \cdot n \cdot RS) \cdot \frac{(q-1)}{2q} \cdot H$$

Where

H = the height of the stow

m = the mass of the stow

$g = 9.81 \text{ m/s}^2$

a_t = transverse acceleration/g

q = the number of tiers of packages in the stow

n = the number of stacks of packages in the stow

f_{RS} = the "RS-fraction factor" ≤ 0.25

RS = the racking strength of a package

3.5 Discussion how to determine the strength of uprights holding timber packages

The goal for this chapter is to find the best rule to determine the strength of stanchions holding timber packages. As said before the dynamics is very complex: tipping, sliding and racking can happen simultaneously. Those three types of dynamics have been examined separately in the three previous sections and three different formulas have been derived.

Neither of these can alone give a true picture of the requirements for the uprights. In order to cover the impact of all dynamics the one rule that will give the highest value in every specific case will be the one to apply.

So given the three rules for tipping (3.2.2), sliding (3.3.3) and racking (3.4.2) respectively:

$$(3.2.2) \quad M_{bt} = \frac{mg}{n} \cdot \left(a_t \cdot \frac{H}{2} - a_v \cdot \frac{b}{2} \cdot r \right) \cdot \frac{1 - (1 - F)^n}{F} \cdot C$$

$$(3.3.3) \quad M_{bs} = mg(a_t - \mu_2 \cdot a_v) \cdot \frac{q-1}{2q} \cdot H \cdot C$$

$$(3.4.2) \quad M_{br} = (m \cdot a_t \cdot g - f_{RS} \cdot q \cdot n \cdot RS) \cdot \frac{(q-1)}{2q} \cdot H$$

the requirement for the bending moment of an upright would be

$$M_b = \max(M_{bt}, M_{bs}, M_{br}).$$

The value of the formula can be divided by the number of stanchions N on the same side and divided by k = 2 if there are chain hog lashings of sufficient strength. Otherwise the coefficient k = 1 if the uprights are not attached to the ones opposite or attached only with elastic web lashings. Finally the factor 1.35 should be added because the uprights may be unevenly affected. And the pressures from the wind PW and from the sea sloshing PS should be added. Then the combined formula gets its final form:

$$(3.5.1) \quad M_b = \frac{1.35}{N \cdot k} \cdot \max(M_{bt}, M_{bs}, M_{br}) + 1.35 \cdot \frac{H}{2 \cdot N \cdot k} \cdot (PW + PS)$$

The additional variables are

N = the number of uprights on each side

k = the "hog lashing coefficient" ($1 \leq k \leq 2$.)

PW = Force from wind pressure in kN

PS = Force from sea sloshing in kN

As an illustration the graphs of all three methods are plotted with the values from corresponding model setups in figures 3.5.1 and 3.5.2. Model 2 seems generally to have the lowest values which can be explained by the fact that horizontal slats were used between the tiers in order for the packages to freely slide without getting stuck. They tie the packages together in an unrealistic way which has resulted in a strong interaction as described in subsection 3.3.4. and thereby probably too low readings in the tests. The Model 2 formula line also lies low which can be explained by the assumptions that were the starting point for the derivation of that particular formula: Neither racking nor tipping was taking into consideration.

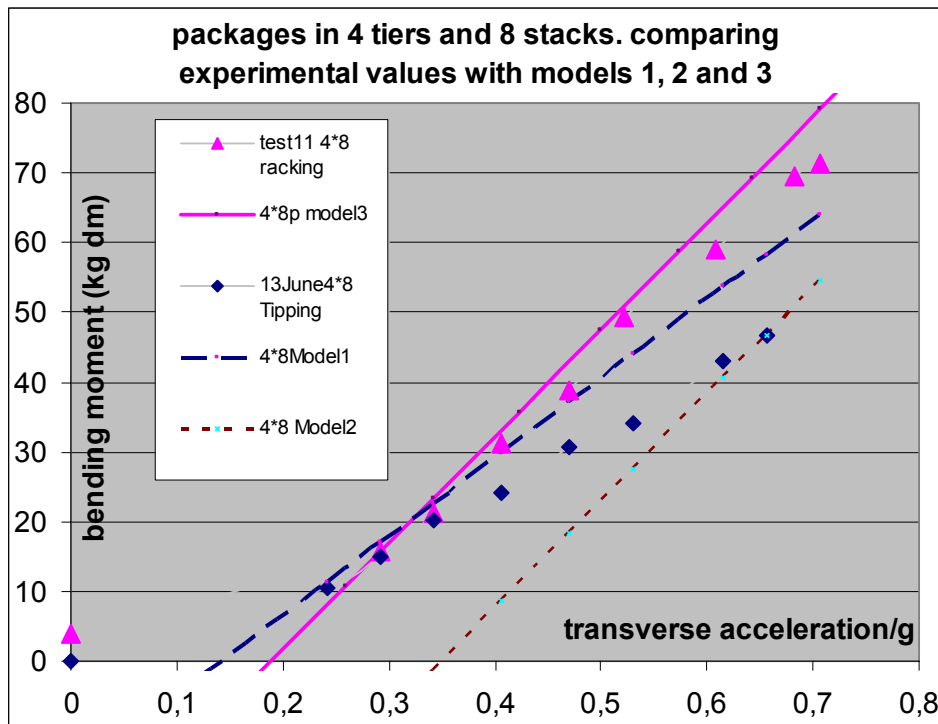


Figure 3.5.1 Experimental values from a model stow of 4*8 packages ($m = 84,8 \text{ kg}$, $H = 4,8 \text{ dm}$) compared with graphs of the three formulas. Corresponding experimental values for transversally sliding packages were not available. The result for this particular example is that Model 1 (with $r = 0.7$ and $C = 1$) should be used for small accelerations and then Model 3 ($RS = 2 \text{ kg}$). Model 2 has $C = 1$ and $\mu_2 = 0.35$.

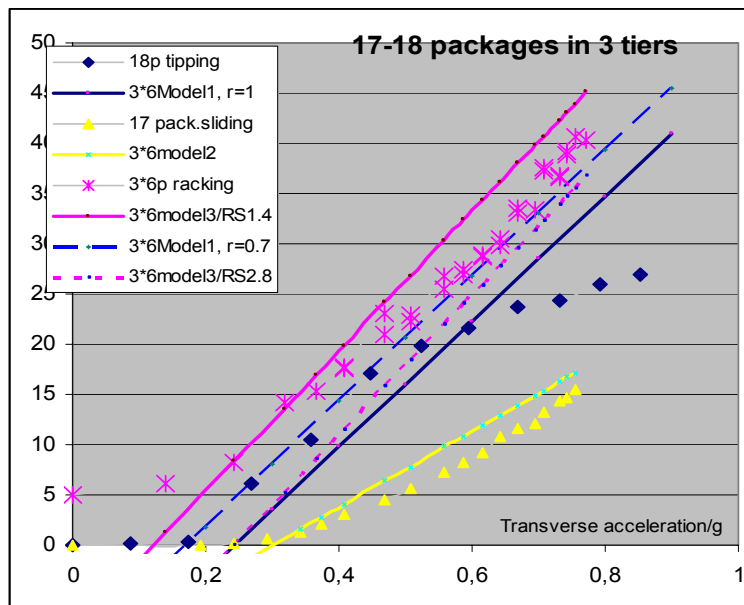


Figure 3.5.2 Model 3 has the highest values all the way. It can be explained by the fact that these y-packages were strapped lightly ($RS = 1.4$) and for the other tests they were deliberately strapped firm. An adjusted model 1 ($r = 0,7$) would fit the points better and a model 3 drawn with $RS = 2.8$ would lie lower than the former. The model 2 points seem always to stay low. The model 2 line has $C = 1$.

4 References

1. P.Anderson, S. Sökjer-Petersen: Practical Tests with Timber Deck Cargoes, MariTerm AB 2008.
2. Veden Engineering AB: Cargo Secure Amendment, MS Nossan, Carriage of pulpwood on weather deck project 2003101, Erik Thun AB.
3. E.Karpovich, O.Karpovich, Y.Voynarovskiy: Russian Design Criteria for Uprights for Sawn Wood.
4. Sjöfartsverkets författningssamling SJÖFS 2003:14.
5. CEN/TC 168/WG 6: Practical inclination test for determination of the efficiency of cargo securing arrangements.
6. S. Sökjer-Petersen: Studiebesök i Longview (USA) och Vancouver (Kanada)

4.1 Special thanks to

- *Peter Andersson* and *Sven Sökjer-Pedersen* of Mariterm AB for good collaboration
- *Björn-Olof Erikson*, captain, lecturer, for assistance and discussions
- *AP Flankkila* and *PA* for helping build the models.
- *Henrik Karlsson*, vice-rector, captain for help in raising funds
- The *Åland University of Applied Sciences* for material and financial support
- The *Maritime authority of Finland* for financial support
- *Sjöfartsstiftelsen i Finland* for financial support
- *Alandia-Bolagen* for financial support
- *Förbundet för Främjandet av Åländsk Sjöfart* for financial support
- *Stiftelsen Hilda och Gustaf Eriksons samt Gustaf Adolf Eriksons understödsfond* for financial support
- *Carl Rundberg AB* for donation of wood for the models
- *Ålands yrkesskola*, house builders programme for preparing the wood.